# Molecular BioSystems

Accepted Manuscript


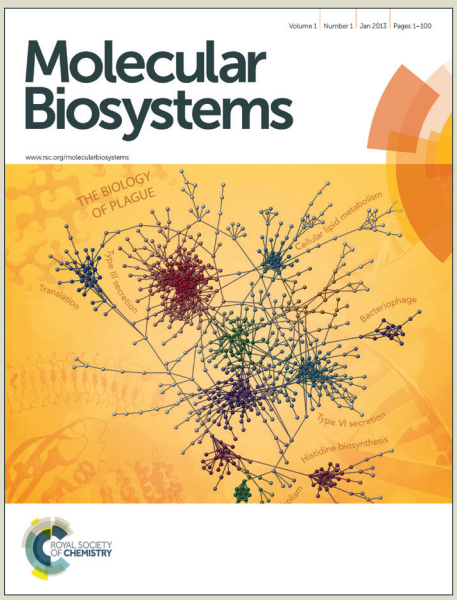





ROYAL SOCIETY OF CHEMISTRY

www.rsc.org/molecularbiosystems

# Temporal-logic Analysis of Microglial Phenotypic Conversion with Exposure to Amyloid-β

Thomas J. Anastasio

*Computational Neurobiology Laboratory*
*Department of Molecular and Integrative Physiology, and*
*Beckman Institute for Advanced Science and Technology*
*University of Illinois at Urbana-Champaign*
*Urbana, IL, USA. E-mail: tja@illinois.edu*

## Abstract

Alzheimer Disease (AD) remains a leading killer with no adequate treatment. Ongoing research increasingly implicates the brain's immune system as a critical contributor to AD pathogenesis, but the complexity of the immune contribution poses a barrier to understanding. Here I use temporal logic to analyze a computational specification of the immune component of AD. Temporal logic is an extension of logic to propositions expressed in terms of time. It has traditionally been used to analyze computational specifications of complex engineered systems but applications to complex biological systems are now appearing. The inflammatory component of AD involves the responses of microglia to the peptide amyloid-β (Aβ), which is an inflammatory stimulus and a likely causative AD agent. Temporal-logic analysis of the model provides explanations for the puzzling findings that Aβ induces an anti-inflammatory and well as a pro-inflammatory response, and that Aβ is phagocytized by microglia in young but not in old animals. To potentially explain the first puzzle, the model suggests that interferon-γ acts as an "autocrine bridge" over which an Aβ-induced increase in pro-inflammatory cytokines leads to an increase in anti-inflammatory mediators also. To potentially explain the second puzzle, the model identifies a potential instability in signaling via insulin-like growth factor 1 that could explain the failure of old microglia to phagocytize Aβ. The model predicts that augmentation of insulin-like growth factor 1 signaling, and activation of protein kinase C in particular, could move old microglia from a neurotoxic back toward a more neuroprotective and phagocytic phenotype.

## Introduction

Alzheimer Disease (AD) is a neurodegenerative disorder of high prevalence that currently is the sixth leading cause of death in the United States (www.alz.org). It has a complex, multifactorial etiology. Clinical and epidemiological evidence increasingly indicates that inflammation plays an important role in AD pathogenesis [1]. The inflammatory response is highly complex in its own right. A large number of experimental observations on specific aspects of the inflammatory component of AD have accumulated, and effectively aggregating these into a format usable for data interpretation and hypothesis generation presents a critical challenge. The purpose of the research described here is to use specialized computational methods to specify the interactions between many of the molecules and cellular processes thought to be involved in the inflammatory component of AD, and then use temporal logic to analyze them. The data-driven specification represents experimental findings as reported, and is course-grained but thorough. Analysis of the model provides new insights into the nature of the inflammatory response in AD and makes several experimentally testable predictions.

The pathological hallmark of the AD brain is the presence of plaques composed of the peptide amyloid-β (Aβ) [2] (see Supplementary Table S1 for all abbreviations). Over accumulation of Aβ is toxic to neurons and is thought to contribute to AD pathology [3]. The inflammatory response in the brain is mediated by microglia, which are the brain's main immune cells and are found in abundance around Aβ plaques [1f, 4]. Among other human AD concomitants, Aβ plaques and brain inflammation are also observed in Aβ-overproducing transgenic-mouse AD models [5].

Epidemiological studies indicate that chronic use of NSAIDs is protective against AD [6], and that the benefit may result mainly from a reduction in brain inflammation due to NSAIDs [7]. Studies using transgenic AD mice show that NSAIDs can reduce soluble Aβ levels and Aβ deposits in brain, and can also reduce microglial activation, levels of pro-inflammatory factors such as IL1β and PGE2, and activation of NFκB [8]. Further experiments in transgenic AD mice reveal that microglia are involved at different stages of the disease process. In early stages, microglia assume a phagocytic state in which they clear Aβ, but in later stages they switch to a cytotoxic state in which they release inflammatory cytokines such as IL1β and TNFα, which are toxic to neurons at high levels [1a].

These results in transgenic AD mice suggest a possible approach to the treatment of AD in which microglia are maintained in the phagocytic phenotype, or even converted from the inflammatory to the phagocytic phenotype. The analysis presented in this paper is focused on a computational assessment of that possibility, and on the cytokines and other factors that regulate microglial phenotype. The details of

the phagocytic process itself are not considered. Although complement components and chemokines also may be involved in AD pathogenesis, they are excluded from the model because their role in microglial activation in AD is not yet clear [1f, 9].

Other potential contributors are also excluded. For example, brain inflammation can lead to infiltration of bone marrow-derived monocytes that could become microglia in the brain, and these could also play a role in Aβ clearance [10], but the conditions under which this occurs are still in question [1f]. A recent pathology study showed that the total number of microglia remains constant over the course of AD in human brain but that the ratio of activated to resting microglia increases, indicating that microglial responses in AD are largely due to a phenotypic conversion of resting microglia rather than to proliferation of microglia or to infiltration of monocytes into brain [11]. Also, T-cells infiltrate the brain in transgenic AD mice at advanced ages [12], and antibodies against Aβ can reduce Aβ load in transgenic AD mice and humans but can also cause meningoencephalitis associated with T-cell infiltration into brain [13]. The potential contribution to the microglial population of infiltrating bone marrow-derived monocytes or other immune cells is not considered here in order to focus on phenotypic changes of brain-resident microglia. Finally, astrocytes, which are the most abundant type of glial cell, also participate in the brain's inflammatory response [14], but their contribution is not considered here in order to focus on the microglial contribution.

The computational analysis presented here revolves around salient and general findings concerning microglial phenotype in the presence of Aβ. The data are derived mainly from experiments in mice. The general observations are that Aβ exposure causes microglia to produce both pro-inflammatory and anti-inflammatory cytokines, that Aβ exposure increases phagocytosis in microglia from "young" mice but decreases it in microglia from "old" mice (roughly less than or greater than one year old, respectively), and that the old, non-phagocytic phenotype is persistent in that it is maintained once it is adopted. Among other results, the analysis suggests that IFNγ might provide an "autocrine bridge" over which an initially pro-inflammatory stimulus such as Aβ could increase production of anti-inflammatory cytokines. It also identifies IGF1 as another autocrine bridge over which the phagocytic state of microglia could potentially be promoted. The model makes predictions of therapeutic relevance on the basis of these findings.

The computational analysis employs techniques from formal methods in computer science [15]. A formal methods analysis of a system is based on a computational representation of that system in a declarative programming language, which offers analysis capabilities not available to programs written in more conventional, imperative languages. Whereas a statement in an imperative language is a command, a

statement (or declaration) in a declarative language is a fact. A declarative program, in which the statements describe the facts concerning the interactions between the elements of the system being modeled, is known as a system specification. The main advantage of specifications written in declarative languages is that they can be used not only for simulation but also can be analyzed using temporal logic and state-space search [16]. When the specification is composed of facts that are true concerning the system, temporal logic analysis and state-space search can be used essentially to prove what else is true for that system.

In principle, a declarative language can be used to specify a system at any level of numerical accuracy, but in practice the temporal-logic capabilities of the declarative environment are facilitated by limiting system elements to integer levels of activation (a course-grained representation). For this analysis, element activations are limited to the integers in the range [0, 10]. Limiting element activations to the Boolean {0, 1} has a long history in systems biology [17], and this approach is undergoing continuous development [18]. Modeling paradigms that limit element activations to integer levels include those based on multivalued logic or Petri nets [19]. Temporal-logic analysis of declarative specifications of biological systems, as implemented here, is a relatively new trend [20]. Logic-based models can capture the essential features of biological system behavior and are appropriate in the many contexts in which the parameters needed for kinetic, differential-equation-based models, such as concentrations and reaction rates, are not known [20-21]. The overall goal of the logic-based approach is to represent a biological system in a course-grained but thorough fashion and to develop, through rigorous analysis, a detailed understanding of the mechanistic events that underlie its behavior.

The focus here is on the system of molecular and cellular interactions that determine microglial phenotype in AD. They are specified using a declarative programming language known as Maude [22]. Maude was designed for modeling and analysis of complex systems. So far Maude has been used mainly to model complex engineered systems such as computer operating systems, internet protocols, and even other programming languages [23]. Some applications of Maude to biological systems have also appeared [24]. Recently, Maude has been applied to problems in AD pathophysiology [25]. This work can be consulted for further background on Maude and on how it can be applied to biological systems.

A declaration in a declarative language specifies how a term matching its left-hand side should be replaced by a term matching its right-hand side. Declarations in Maude are of two types:

equations and rules. Equations elaborate the current state of the system model while rules transition the system from one state to another. Maude performs search and temporal-logic analysis of system models by first generating the entire state-transition tree, taking all possible trajectories through the state space and finding all possible terminal states (a.k.a. steady states). Then state-space search is used to find specific states of interest, while temporal-logic analysis is used to verify time-qualified propositions such as whether a specific state always occurs, eventually occurs, does not occur until another specific state occurs, and so on.

For the microglia system model, the declarations describing autocrine updates (i.e. updates of microglial receptors to factors generated by the microglia themselves) are expressed as rules. All other declarations are expressed as equations. In this way the state of the microglia system model is advanced each time one of its receptors is updated by a self-generated factor. This approach facilitates analysis of the microglia system and leads to potential new insights into the behavior of microglia in the AD brain.

## Experimental background and model construction

The model is based on molecular and cellular interactions as determined through focused laboratory-based experiments and as described in the literature. Only statistically significant interactions are included in the model. The next subsection describes in detail the experimental findings on which the model is based, while the subsection following describes construction of the computational model.

### Biological interactions represented in the model

Microglia are endowed with a large variety of receptors and receptor complexes and can be induced, via signaling cascades proceeding from them, into inflammatory or phagocytic phenotypes [4]. The specific phenotype they assume is most likely determined by the combination of receptors that are activated, which in turn is determined by the ligands that are present, which in turn is determined by the state of the organism. A large literature implicates Aβ as a key ligand in the AD brain.

Aβ tends to self-aggregate into soluble oligomers of low order, into fibrils, and into plaques [26]. Microglia respond to and phagocytize mainly fibrillar Aβ (fAβ). Fibrillar Aβ binds to a microglial receptor complex (the TLR complex) composed of the Toll-like receptors TLR2 and TLR4, along

with the co-receptors SRA, CD14, CD36, CD47, and the α6β1 integrin [27]. Activation of the TLR complex leads to phosphorylation of the Src, Lyn, and Syk kinases in microglia in culture [28]. Lyn and Syk can both phosphorylate Vav, and Vav can then load a GTP onto the GTPase Rac [29]. Rac is also part of the NADPH oxidase complex, and Rac activation can lead to the production of ROS by the NADPH complex [30].

TLR2 and TLR4 also signal through the adaptor protein MyD88, and TLR4 separately signals through the TRIF protein [4b, 27b]. MyD88 activates IRAK, and IRAK associates with TRAF6 [31]. TRAF6 activates TAK1, and TAK1 then activates IKK, which inactivates IκB, which releases and thereby activates NFκB. TAK1 also activates MAP3K, which activates MAP2K, which activates MEK. MEK activates ERK, as well as p38MAPK and JNK, leading to activation of AP1. Independently of MyD88, TLR4 also activates TRIF, which activates RIP1, and RIP1 also activates TAK1. Thus, the MyD88/TRAF6 and TRIF/RIP1 pathways are parallel pathways leading to activation of TAK1 [4b]. Activation of NFκB or AP1 promotes expression of pro-inflammatory mediators [27d].

Activation by fAβ of the TLR complex can cause various microglial reactions, which depend on factors that in turn depend on age. Experiments using transgenic AD mice that are also deficient in TLRs show that Aβ activation of TLR2/4 reduces Aβ load as the mice age, and increases production of pro-inflammatory cytokines such as IL1β, IL17, and TNFα but can also increase production of anti-inflammatory cytokines and other factors such as IL10 and TGFβ [32]. TGFβ signals through its receptor TGFR and transcription factors known as Smad proteins [33]. TGFβ promotes Aβ phagocytosis by microglia [34]. In transgenic AD mice with normal TLRs, microglia transition from a phagocytic form at age 6 months (young) to the classic, cytotoxic form at age 18 months (old) [12]. The switch is coincident with high levels of Aβ and of inflammatory mediators including IL1β, TNFα, NADPH oxidase, and COX2. Although expression of the tissue-repair factor Arg1 is not increased, levels of the related factor Ym1 are increased in young transgenics while the anti-inflammatory IL4, IL10, and TGFβ are increased in old transgenics [12]. These results indicate that microglia in transgenic, Aβ-overproducing mice start out phagocytizing Aβ but end up becoming predominantly inflammatory and cytotoxic, and this compromises their ability phagocytize Aβ.

Studies in which levels of inflammatory cytokines are increased in mice, either through genetic overexpression or direct administration, show that augmentation of inflammatory cytokines can

actually promote Aβ phagocytosis in young mice but suppress it in old mice. Local brain (hippocampal) overexpression of IL1β in young wildtype mice increases production of IL1β, IL6, and TNFα, while in young transgenic AD mice, local overexpression of IL1β actually reduces the Aβ load [35]. Administration of IL6 induces a microgliosis that reduces Aβ deposition in young AD transgenic mice [36]. However, as the mice age, increasing levels of inflammatory cytokines such as IL1β, IL6, and TNFα lead to decreasing phagocytic ability in microglia [37]. Transgenic AD mice that lack the pro-inflammatory IL12 and IL23 have a lower Aβ load than do the same mice that have normal levels of IL12 and IL23 as they age [38]. The inflammatory effects of IL1β are suppressed to some extent by the naturally-occurring IL1 receptor antagonist IL1Ra [39]. These results suggest that in young mice, inflammatory cytokines actually induce microglial phagocytosis of Aβ but in old mice, inflammatory cytokines induce a more cytotoxic microglial phenotype with suppressed phagocytic ability.

Studies using isolated microglia in culture paint a similar picture. In microglia from young mice, activation by fAβ leads to ROS production and phagocytosis, and this is attenuated, but not eliminated, in Vav knockout microglia [29]. IL6 induces microglia from young mice to increase Aβ phagocytosis and to increase Ym1 but not Arg1 [36]. IL6 signals through STAT3 via the IL6 receptor IL6R and JAK2 in certain cell lines [40] and possibly also in microglia. TNFα induces microglia from young mice to increase Aβ phagocytosis [41]. In contrast, in old mice, microglia produce more IL1β and TNFα and phagocytize less Aβ [37b]. Binding of fAβ to the TLR complex in the N9 microglial cell line causes an increase in IL1β and IL6 [42]. These results indicate that Aβ or inflammatory cytokines can increase phagocytosis by microglia in young brains but decrease it in old brains.

IL4 emerges from studies of microglia in culture as a factor potentially useful for maintaining microglia in a phagocytic state, while IFNγ presents a mixed picture. In one study, fAβ causes neonatal microglia to increase TNFα but to decrease the anti-inflammatory IGF1. This pro-inflammatory response is blunted if microglia are pretreated with IL4 or, to a lesser extent, with IFNγ [43]. By itself, IL4 increases IGF1 and decreases TNFα while IFNγ does the opposite. Pretreatment with Aβ does not alter IL4-induced IGF1 expression. Taken together, these results show that IL4 is much better at preserving the neuroprotective state than IFNγ, while IFNγ has mixed but interesting properties. Antibodies against IGF1 significantly weaken the neuroprotective effect of IL4, suggesting that IL4 exerts its effect mainly through IGF1 [43].

In a related study, IFNγ is shown to stimulate secretion of TNFα and production of iNOS from wildtype microglia isolated from old mice, but not from microglia from mice with the interferon receptor IFNR knocked out [44]. However, fAβ causes IFNγ secretion from microglia independently of IFNR. IL4 signals through STAT6 via the IL4 receptor (IL4R) and JAK1 [45], while IFNγ signals through JAK2/STAT1 [46]. IGF1 reduces ROS and TNFα production by inflammatory microglia, and these effects are thought to result from activation of the IGF2 receptor IGF2R and/or a hybrid of the insulin receptor IR and IGF1R (IRIGF1R) [47]. IGF1, IGF2, and insulin each have affinity for IGF1R, IGF2R, IR, and IRIGF1R [48]. Activation by IGF1 of IRIGF1R could reduce ROS via the pathway PI3K to Akt to FOXO to SOD, while activation by IGF1 of IGF2R could reduce TNFα via the pathway Gq to PKC [48].

Several studies applied the endotoxin LPS to microglia in culture to explore inflammatory reactions and changes in Aβ phagocytosis. LPS binds with the TLR complex and in low doses can induce the phagocytic microglial phenotype [49]. At higher doses, LPS causes microglia isolated from young mice to substantially increase their production of the pro-inflammatory cytokines TNFα, IL1β, IL6, and IL12, and to increase the anti-inflammatory IL10 [50]. These results are largely confirmed and extended in a more recent study that employs a more stringent isolation technique [51]. LPS causes pure postnatal murine microglia to increase production both of TNFα and TGFβ. Also in these microglia, TGFβ production is increased by TNFα but TNFα production is decreased by TGFβ. Like LPS, IFNγ causes these microglia to increase production both of TNFα and TGFβ (the reported TGFβ increase was not significant). LPS causes microglia isolated from neonatal rats to decrease production of IGF1, but LPS does not substantially diminish the increase in IGF1 produced by IL4 [43]. BV2 (immortalized murine microglial cell line) microglia reduce their level of Arg1 production when exposed to high dose LPS [52].

In comparison with young microglia, exposure to LPS of microglia isolated from old mice causes them to produce even more TNFα, IL1β, IL6, and IL12 [50]. Old microglia do not decrease TGFβ production with LPS exposure but they actually produce more IL10. Activation of microglia using LPS and fAβ promotes a predominantly inflammatory phenotype and synergistically increases secretion of IL1β and decreases secretion of IL4 [1d]. Pretreatment using LPS or pro-inflammatory mediators including IL1β, TNFα, or IFNγ inhibits the fAβ-induced phagocytosis of fAβ by primary murine or BV2 microglia [53]. The resulting pro-inflammatory suppression of phagocytosis can be relieved by NFκB inhibitors, by the anti-inflammatory cytokines IL4, IL10, IL13, and TGFβ, by COX2 inhibitors such as NSAIDs, or by an antagonist of the prosthanoid receptor EP2.

Ablation of EP2 substantially suppressed microglial production of the pro-inflammatory mediators iNOS and COX2, and enhanced Aβ phagocytosis by microglia [54]. The enhancement of phagocytosis by EP2 ablation is completely prevented by inhibition of PKC, suggesting that EP2 normally suppresses microglial phagocytosis by inhibiting PKC.

Several studies point to PPARγ as a key player in the determination of microglial phenotype and as a mediator of the beneficial effects of NSAIDs, since NSAIDs increase PPARγ expression [55]. If initiated while the animals are still young, treatment of transgenic AD mice with the NSAID ibuprofen reduces IL1β, both soluble and aggregated Aβ, and the number of pro-inflammatory microglia [8a]. Similar treatment of transgenic AD mice with ibuprofen also reduces Aβ plaques and expression of COX2 and iNOS, while treatment with the PPARγ agonist pioglitazone does the same but to an even greater extent [56]. Rosiglitazone, another PPARγ agonist, reduces IL1β, iNOS, and NO but increases IL4 in the hippocampus of old rats [57].

PPARγ forms a heterodimer with RXR before binding PPAR response elements and opposing NFκB but promoting expression of anti-inflammatory mediators. Both pioglitazone and the PPARγ modulator DSP-8658 enhanced the phagocytosis of Aβ by microglia [58]. Retinoic acid or bexarotene, which are both RXR agonists, also enhance microglial Aβ phagocytosis.

LXRβ also forms a dimer with RXR, and LXRβ knockout increases Aβ load in AD transgenic mice [59]. Ligands of LXRβ suppress development of the pro-inflammatory phenotype and contribute to the maintenance the phagocytic phenotype in microglia exposed to fAβ. Ligands of LXRβ also suppress LPS- or IL1β-induced production by microglia of iNOS, NO, COX2, TNFα, and of IL1β itself, and reverse the inhibition by LPS or IL1β of fAβ-induced Aβ phagocytosis by microglia. These data suggest that LXRβ demotes the inflammatory and promotes the phagocytic phenotype in a manner similar to that of PPARγ. Also, NaHS, a donor of H2S, reduces Aβ-induced microglial production of IL1β, IL6, TNFα, and COX2 by inhibiting the activation of NFκB [60]. Though PPARγ opposes NFκB, NFκB can also oppose PPARγ. In macrophages, activation of TLR2/4 reduces PPARγ expression at the mRNA level, but this is prevented by inhibition of IKK or NFκB [61]. NFκB-induced reduction in PPARγ expression is associated with increased production of pro-inflammatory cytokines including TNFα. These findings reveal a mutually antagonistic interaction between PPARγ and NFκB in macrophages.

An important class of modulators of microglial phenotype are factors attached to or secreted by neurons, and some of these counter the anti-inflammatory, phagocytic phenotype. The CD40 ligand CD40L suppresses the phagocytic response to fAβ of BV cells or of primary murine microglia [53]. Knockout of the CD40L gene in transgenic AD mice results in reduced Aβ plaques and reduced microgliosis and TNFα expression [62]. Microglia derived from neonatal rats take up more Aβ when pretreated with IL4 if they do not express CD40 [63].

Conversely, most of the neuronal membrane-bound or secreted factors seem to maintain microglia in the phagocytic state. Recent genomewide association studies show that homozygous loss-of-function mutations in the gene encoding TREM2 are associated with a significant risk for AD [64]. The TREM2 ligand TREM2L is expressed on neural membranes [65]. TREM2 signals via DAP12 [66]. Activation of TREM2 phosphorylates DAP12, which provides a docking site for Syk. Syk promotes phosphorylation of GRB2, which leads to activation of ERK, which in turn leads to reorganization of the cytoskeleton and increased phagocytosis in microglia [65a, 67]. Myeloid precursor cells (which can become microglia) that overexpress TREM2 show increased phagocytosis, but this is blocked by inhibition of ERK [68]. They also produce more IL10, but less of each of IL1β, iNOS, TNFα, and IFNγ. Knockdown of TREM2 in microglia inhibited phagocytosis and increased production of TNFα, IL1β, IL12, and iNOS. Stimulation by ligands of TLR2 (which include Aβ) leads to inhibition of TNFα production by microglia, but only if TREM2 is available to phosphorylate DAP12 [69].

Other membrane-bound factors that help keep microglia in a neuroprotective state include CD22 and CD200 [65b]. The neuronal membrane-bound CD45 ligand CD22, which can also be secreted by neurons in soluble form, inhibits LPS-induced TNFα secretion by microglia [70]. Neurons express CD200 while microglia express the CD200 receptor CD200R [71]. CD200 expressed on neurons significantly attenuates Aβ-induced secretion by microglia of IL1β, IL6, and TNFα. In mouse bone marrow-derived mast cells, activation by CD200 of CD200R inhibits signaling via the ERK, JNK, and p38MAPK pathways [72]. Binding of CD200 to CD200R causes CD200R phosphorylation and binding of CD200R to docking proteins Dok1 and Dok2. Dok1 binds SHIP1 and both Dok1 and Dok2 recruit GAP. GAP then inhibits Ras. Since Ras activates ERK, CD200/CD200R inhibits ERK via this mechanism. How CD200R inhibits JNK and p38MAPK is not known. CD200 expression decreases with age and also decreases as a result of Aβ application, and both CD200 and CD200R expression are reduced in the human AD brain, specifically in the hippocampus and cerebral cortex [73].

Fractalkine is enigmatic in that it seems to promote either microglial phenotype, depending on circumstances. Fractalkine (a.k.a. CX3CL1) is expressed by neurons throughout the brain and can exist either in membrane-bound or soluble form [74]. Deficiency of the fractalkine receptor CX3CR1 causes microglia to become neurotoxic [65b, 75]. This result suggests that fractalkine promotes the neuroprotective, phagocytic phenotype. However, transgenic AD mice have reduced Aβ deposition and increased Aβ phagocytosis if they are also deficient via gene knockout in CX3CR1 [76]. The CX3CR1 deficiency decreases production of TNFα, but increases production of IL1β, by microglia in transgenic AD mice. In culture, CX3CL1 reduces phagocytosis of Aβ by microglia [76]. Thus, fractalkine is like IFNγ in that it can promote either the neurotoxic or the neuroprotective phenotype, but in suppressing IL1β while enhancing TNFα its effects are even more ambiguous. Transgenic AD mice produce fewer fractalkine positive cells than wildtype when younger but fractalkine levels decrease in both and even out when older [77].

While healthy neurons express proteins that suppress the pro-inflammatory microglial phenotype, necrotic neurons express proteins that enhance it. Necrotic neurons, but not other necrotic cell types, can induce the pro-inflammatory phenotype of microglia through a signaling cascade involving MyD88 [78]. Microglia induced by necrotic neurons have increased production of IL6, IL12, TNFα, NO, CD40, and α6β1 integrin.

Another factor important for the determination of microglial phenotype in AD is ACh. AD is associated with loss of cholinergic neurons early in the disease process [79]. Microglia express the ACh receptor α7nAChR [80]. Pretreatment with ACh or nicotine inhibits the LPS-induced release from microglia of TNFα [80a, 81]. This inhibition is mediated by a reduction in phosphorylation of p38MAPK and JNK [82]. The mechanism is not known but it appears to occur without the influx of extracellular calcium [81, 83]. Activation of α7nAChR by nicotine also reduces ROS production by preventing NADPH activation [83]. Donepezil, a widely used anticholinesterase, attenuates the Aβ-induced release of the inflammatory mediators IL1β, TNFα, PGE2, and NO, and reduces the upregulation of iNOS and COX2, the phosphorylation of p38MAPK, and the activation NFκB in microglia [84]. The interactions outlined in this subsection are diagrammed in Figure 1 and specified computationally as described in the next subsection. Data from this subsection that are used to verify the model are summarized in Table 1.

**Computational representation of microglia signaling**

Computational representation of the microglia signaling system begins by representing its constituent molecules (and some cellular processes) as elements of the model, and proceeds by specifying the interactions between those elements. The main focus of this analysis is on a specification of the microglia system in a declarative programming language (Maude) but for purposes of providing a cross-check, the same interactions are also represented in an imperative language (MATLAB). Model elements in the Maude and MATLAB versions have the same names. To distinguish them from biological entities, model element names are rendered in `monotype` font (see Table S1). Because model element names correspond to program variable names they substitute lower-case Roman letters for Greek letters.

The model is based on data derived from experiments using molecular biology techniques (e.g. gel electrophoresis, immunohistochemistry, phagocytosis assay, etc.) that provide relative measures of molecular abundance or activity rather than precise chemical concentrations or reaction rates. For this reason, all model elements are assigned integer levels in the range [0, 10] that represent their relative activity. In Maude all elements are represented as operators that assign an integer level to the element they represent, while in MATLAB all elements are represented simply as variables. For example, in Maude the operator `IL1b(7)` assigns the level 7 to `IL1b` while in MATLAB the variable `IL1b` simply would be set to 7. The slightly more complicated representation in Maude is a requirement of its analytical capabilities.

Declarations in Maude are either equations or rules. Applicable equations must execute but applicable rules may execute or not, and all equations must execute before any rule can execute (see also Introduction). All of the declarations in the Maude specification, and all of the statements in the MATLAB program, describe how the level of one model element is changed by the levels of certain other model elements. For example, in Maude:

```
MyD88(X1) IL1R(X2) IRAK(Y) =
MyD88(X1) IL1R(X2) IRAK(X1 + X2) if Y =/= X1 + X2 .
```

While in MATLAB:

```
if IRAK ~= MyD88 + IL1R, IRAK = MyD88 + IL1R;
upFlag = 1; end
```

Both constructions prescribe that the level of `IRAK` should be equal to the sum of the levels of `MyD88` and `IL1R`. Both are also conditional, so that the level of `IRAK` will not be reassigned if it

is already equal to the sum of the levels of `MyD88` and `IL1R` (note that =/= and ~= mean "not equal" in Maude and MATLAB, respectively). This declaration is an equation in Maude, so it executes whenever it applies. If either the level of `MyD88` or `IRAK` changes over the course of simulation or analysis, then this equation will execute and change the level of `IRAK`. In contrast, in MATLAB a statement executes according to its order in the program. To make the Maude and MATLAB version operationally more similar, all of the statements in the MATLAB version occur within a while loop that first sets `upFlag` to 0 and that breaks only if none of the conditionals in the loop execute and set `upFlag` back to 1. In other words, if any conditional executes then all of the conditionals must be checked again before the MATLAB simulation can terminate. Almost all declarations/statements in both the Maude and MATALB versions are conditional. The only ones that are not are those that assign the initial levels of the pro- and anti-inflammatory cytokines in the model.

In the Maude version almost all of the declarations are equations. The ones that are rules rather than equations are those that specify the autocrine interactions, or the levels of the receptors for the pro- and anti-inflammatory factors that are generated by the microglia system itself. A rule in Maude takes the same form as an equation except that the = sign is replaced with =>. The model represents 78 interactions among 107 elements including initial and constitutive levels of some elements that are not shown in Figure 1. In the Maude version, 9 of these interactions are the rules that set the 9 autocrine receptor responses. Besides being expressed in different languages, all of the interactions are the same in the Maude and MATLAB versions and most of these are very simple. Elements that receive input from one other element simply take the level of their input element. Many other elements receive input from two or three other elements and for these the interaction is either a simple sum or difference (bound at 0) or a max operation. Only 12 of the 78 interactions are more complex, and these determine the activation of an element on the basis of the pattern of its 3 or more inputs.

The most important operational feature of the model is that the interactions that determine autocrine receptor updates occur last, after the levels of the cytokines and other factors generated by microglia are changed due to other model interactions. This feature in assured in Maude by expressing all autocrine receptor updates as rules, with all other interactions expressed as equations, and in MATLAB by locating all autocrine receptor updates at the end of the while loop that lists all the interactions. Because the microglial autocrine receptors can be activated by factors that microglia themselves produce, the autocrine receptor updates mediate positive-

feedback interactions. In the model these feedback loops are governed by two saturation levels, designated as `proSat` and `antiSat`, which determine the maximal level reachable in any model state by the pro- and anti-inflammatory mediators, respectively. The levels of `proSat` and `antiSat` are determined by the levels of the transcription factors in the model, which are determined, in turn, by the signaling cascades that proceed from the receptors for autocrine mediators and also for exogenous factors. The model reaches terminal states (a.k.a. steady states) when the autocrine mediators reach and hold their saturation levels.

It is important to point out that the model is not the product of a machine learning algorithm in which its structure assumes some standard, homogeneous, *a priori* form (e.g. belief network) and an algorithm is used to fit model parameters. On the contrary, model structure is heterogeneous and custom built according to experimental results and in order to bring overall model behavior in line with observation. In this regard the creation of the microglia signaling model is similar to the creation of models of engineered systems in that the Maude specification is set by the modeler on the basis of knowledge of the system being modeled (a.k.a the target system). The specification is considered valid if its behavior corresponds to that the target system, and analysis of the specification then leads to potential understanding of the target system.

## Results and discussion

The results are derived mainly from temporal-logic analysis and state-space search of a declarative specification of the signaling, transcriptional, and other interactions that determine microglial phenotype in AD. These computationally intensive analysis and search processes, which are characteristic of declarative models, involve generation of the entire state-transition tree by taking all possible trajectories through the state space. Most imperative models, in contrast, take only one, arbitrary trajectory so that computations will be efficient. Because the two modalities are so different it was useful to create both a declarative and an imperative version of the microglia system model and to use the one to check the other. The same interactions were represented in Maude (declarative) and MATLAB™ (imperative). Maude was used in simulation mode for comparison with MATLAB, in which simulation is the only mode. The two versions produced the same output for all inputs (when Maude produced two terminal states, one of those states always matched the MATLAB output; see next subsection). Prerequisite to model analysis is verification that overall model behavior is consistent with observation.

**Overall model behavior**

The salient and consistent findings from the literature are summarized in a truth table (Table 1), which shows what is true for the microglia system given these findings. Because available data are qualitative, the findings are expressed in terms of quantized integer levels. The truth table is organized in terms of certain key model elements designated as inputs and outputs. It is also divided into two parts: the top and bottom parts pertain to brain-resident (*in vivo*) or isolated (*in vitro*) microglia from young or old animals, respectively. Isolated microglia pretreated with Aβ or with inflammatory mediators are considered old for the purposes of the truth table. In the model, the young and old cases differ in that in the young case the factors `ACh`, `CD22`, `CD200`, `CX3CL1`, and `TREM2L` are present but in the old case they are absent. These factors are not completely absent in aging brains but assigning them only two levels, 0 in old and 1 in young brains, is sufficient for the purposes of the model. Obviously other factors also differ between young and old animals. These factors can be added to the model as they are identified experimentally.

For the truth table (Table 1), the inputs are the inflammatory stimuli `Ab` and `LPS`, the initial cytokine levels `IFNgini`, `IL4ini`, and `IGF1ini`, and the signaling modifiers `rosi` and `retino`. The initial cytokine levels are held at 5 or augmented to a level of 8. While some Aβ is normally present in young and old brains, the input `Ab`, like the inputs `LPS`, `rosi`, and `retino`, is limited to levels of 0 and 1 for simplicity in the model. Each input pattern is associated with one (sometimes two) terminal output patterns. The outputs are the pro-inflammatory factors `IL1b`, `TNFa`, and `ROS`, the process `phago`, and the anti-inflammatory mediators `Ym1`, `Arg1`, `IL4`, `IL10`, `TGFb`, and `IGF1`. For the outputs in the truth table, boldface numerals designate an experimental observation that the model had to match. These observations are assigned the integer levels of 3, 5, and 7, corresponding to `low`, `base`, and `high`, respectively. Within the constraints established by known interactions, model creation was focused on bringing its overall input/output behavior into agreement with these observations. The chosen set of inputs and outputs is obviously not an exhaustive set of the factors to which microglia respond and that they produce, but they are the factors most often examined in experiments on Aβ effects on microglia.

Both the Maude and MATLAB versions of the model agreed with each other and with the boldface numerals in the truth table. Agreement of both versions with the data on the effects of Aβ on microglia indicates that the model can be considered as a valid representation of the microglia system. Agreement between the Maude and MATLAB versions provides assurance that agreement with the data is not due to programming error. On the output side of the truth table, plain numerals are model outputs for which no corresponding experimental observations yet exist. All of those can be considered as model predictions.

In constructing the truth table, Maude was run in search mode in order to determine the terminal states of all possible trajectories through the state space. Because the rules in the model expressed autocrine receptor updates, each trajectory represents one of the possible sequences of updates of the autocrine interactions. The truth table (Table 1) shows that, starting from most of the initial states with inputs as specified, the specification reached only one terminal state, meaning that the same state was reached no matter the order of updates of the autocrine interactions. However, that truth table has two paired rows, 5a/5b and 10a/10b, that show two different outputs for the same initial input state. These are the outputs of two stable (a.k.a. terminal) states of the Maude specification for initial states with augmented initial levels of `IL4` (i.e. `IL4ini(8)`). The fact that these initial states give rise to two separate terminal states is of significance for the analysis (see below). The MATLAB version, in contrast, reaches only one terminal state from all initial states because it takes only one, arbitrary trajectory through the state space.

For the two paired rows of the truth table, 5a/5b and 10a/10b, the initial level of `IL4` is augmented (i.e. `IL4ini(8)`) but the initial levels of `IFNg` and `IGF1` are at the `base` level (`IFNgini(5)` and `IGF1ini(5)`) (Table 1). Also, both `rosi` and `retino` are absent (`rosi(0)` and `retino(0)`). For the row pair 5a/5b, the model is in the young condition and `Ab` and `LPS` are both absent (`Ab(0)` and `LPS(0)`). For the row pair 10a/10b, the model is in the old condition and both `Ab` and `LPS` are present (`Ab(1)` and `LPS(1)`). The output numerals in the first member of each pair (5a or 10a) are Italic to signify that they represent the Maude terminal states that disagree with the relevant observations. The output numerals in the second member of each pair (5b or 10b) agree with the relevant observations. Although they start from very different initial states, the "correct" terminal states (Table 1 Rows 5b and 10b) in these cases are very similar. The importance of these states can be appreciated in the context of the other truth table input/output patterns.

For the baseline condition in young microglia, `Ab`, `LPS`, `rosi`, and `retino` are all absent and `IFNgini`, `IL4ini`, and `IGF1ini` are all at `base`. The model was arranged so that, in the young case, all the pro- and anti-inflammatory mediators and phagocytosis were at the `base` level, which is 5 (Table 1 Row 1). All experimentally observed baselines were assigned the level of 5 also, and so all of the `base` output levels in this condition are bold in the truth table. If experimental results indicated a significant increase, decrease, or no change in an output for a specific condition and initial input, then that output takes a bold 7, 3, or 5 (corresponding to `high`, `low`, or `base`) in the truth table (Table 1).

Many studies indicate that exposure to Aβ will cause young microglia to increase Aβ phagocytosis and production of pro-inflammatory mediators. Paradoxically, Aβ exposure will also cause young microglia to increase production of anti-inflammatory mediators, the main exceptions being Agr1, which is not affected by Aβ, and IGF1, which is actually decreased by Aβ. Largely the same pattern of changes is observed with LPS exposure, and the model agrees with these findings (Table 1 Rows 2 and 3). Starting from baseline, experimental studies show that an initial augmentation in IFNγ will increase TNFα but decrease IGF1, while an initial augmentation in IL4 will decrease TNFα but increase IGF1. The model reproduces these findings (Table 1 Rows 4 and 5b), and suggests that augmented initial IFNγ produces a microglial state similar to that produced by Aβ or LPS, while augmented initial IL4 can produce a state in which pro-inflammatory mediators are decreased, phagocytosis is increased, and most anti-inflammatory mediators including IGF1 are increased in young microglia.

These facts may be key to understanding microglial phenotypic conversion with exposure to Aβ in young animals. They suggest that IFNγ may allow an inflammatory stimulus such as Aβ to cause increased production of anti-inflammatory mediators also. The fact that IGF1 is often but not always decreased when other anti-inflammatory cytokines including IL4 are increased suggests a special role for IGF1. The fact that the Maude version of the microglia model has two stable states starting from augmented initial `IL4`, in only one of which is `IGF1` increased, suggests that states with increased IGF1 may be difficult for microglia to achieve.

The baseline condition in old microglia is the same as that in young microglia except that old microglia lack `ACh` and other neuronal membrane-bound or secreted factors that are present in the young condition. Experimental studies show that old microglia have increased production of pro-inflammatory cytokines but decreased phagocytosis. The model agrees with these findings (Table 1 Row 6) and suggests that production of certain anti-inflammatory mediators may also be increased in old microglia (see below). Experiments also show that exposure of old microglia to Aβ or LPS separately causes increased production of pro-inflammatory and many anti-inflammatory mediators (Table 1 Rows 7 and 8) and the response is similar to that of young microglia (Table 1 Rows 2 and 3) except that phagocytosis is decreased in the old case.

*In vitro* it is possible to produce a microglial phenotype in which pro-inflammatory cytokines are increased while most (if not all) anti-inflammatory factors are decreased. Specifically, exposure of old microglia to Aβ and LPS *together* causes increased pro-inflammatory but decreased anti-inflammatory cytokine production. Interestingly, this hyperinflammatory condition as well as the less inflammatory

conditions can be reversed by augmented initial IL4, by augmented IGF1, or by compounds such as rosiglitazone or retinoic acid that enhance IGF1 signaling. The model reproduces this set of findings (Table 1 Rows 7-13). Again, the fact that the Maude version has two stable states starting from the old and hyperinflammatory condition and augmented initial `IL4`, in only one of which are pro-inflammatory mediators decreased but anti-inflammatory mediators increased (Table 1 Rows 10a and 10b), suggests that reversal of a potentially hyperinflammatory phenotype in old microglia exposed to Aβ may be difficult to achieve. The behavior of the model in all of these cases is explored in detail throughout the rest of this section.

**Response to Aβ in the young condition**

After the consistency of overall model behavior with observation is established, temporal logic is used to analyse it. In Maude this is done by defining certain properties and then checking whether time-qualified propositions involving those properties are true or false, given specific starting conditions. For example, the property `IL1bEQ7` is true when the level of `IL1b` is 7 (`IL1b(7)`). Note that 7 corresponds to the `high` activity level. Then `[] IL1bEQ7`, where `[]` is the temporal-logic operator "always", is the proposition that `IL1b` is always active at the `high` level. Thorough understanding of model behavior can be developed by using Maude to determine under what conditions this and other propositions are true.

Table 2 presents a temporal-logic analysis of the model in the young case when `Ab` is also present (`Ab(1)`). In this case `IL1b` is always active at the `high` level. It is useful to reiterate here that the only rules in the Maude specification are those that update the levels of the receptors for the factors that are produced by microglia. In other words, only the autocrine interactions are expressed as rules; all other interactions are expressed as equations. In Maude, equations only elaborate the state, they do not change the state of the model. In contrast, rules do change the state, and the state transitions produced by rules are the events that advance the state and produce sequential orderings among different states. If `IL1b` is always active at the `high` level in the presence of `Ab`, then it is brought to that level by equations made applicable by `Ab(1)` right from the start. If `IL1b` is always `high` with `Ab(1)`, then `Ab(1)` brought `IL1b` to this level through execution of equations and before execution of any rules, even if some or all of the rules are also made applicable by `Ab(1)`.

This analysis will feature `IL1b` as representative of pro-inflammatory cytokines, and will also feature `IFNg` due to its importance in autocrine interactions. Likewise it will feature `IL4` as representative of anti-inflammatory cytokines, but will also feature `IGF1` because of its unique and important role.

Featuring IL1b and IL4 as representative is done to simplify presentation of modeling results, not to imply that IL1β and IL4 always behave in lockstep with, respectively, other pro- and anti-inflammatory cytokines. For the model in the young case and in the presence of Ab (Ab(1)), IL1b and IFNg are both always high (Table 2 Row 1), and NFkB is likewise always high, signifying a high level of nuclear translocation (Table 2 Row 2). This indicates that IL1b and IFNg are made high directly through signaling via the TLR complex and NFkB without autocrine interaction in the model. The lack of autocrine involvement in this case is *not* a critical feature of the model and could easily be changed if new data suggest that Aβ requires autocrine amplification in order to produce an inflammatory response. In contrast, signaling pathway structure *is* a critical model feature, and autocrine interactions figure prominently in the mechanism by which Ab regulates anti-inflammatory cytokines in the model.

In the young case and with Ab(1), IL4 is not always high and IGF1 is not always low, but they both "eventually" reach those levels (Table 2 Rows 3 and 4). A signaling molecule of importance in anti-inflammatory regulation is PPARg, but the PPARg level never rises above base in this case (Table 2 Row 5). In contrast, STAT1 and STAT6 are not always but eventually become high (Table 2 Rows 6 and 7), indicating that they require autocrine activation in the model. The changes in IL4 and IGF1 due to Ab are due not to STAT6 but to STAT1, since IL4 is not high and IGF1 is not low "until" STAT1 is high. Furthermore, STAT1 being high "implies" that IL4 is high and IGF1 is low (Table 2 Rows 8-10). This shows that Ab regulation of IL4 and IGF1 depends on signaling through JAK2 and STAT1, which are activated through autocrine interactions involving IFNg and IL6, and the question arises as to whether both are necessary or only one or the other.

This question is best answered using state-space search. In the young case with Ab(1), IL4 is high, IGF1 is low, and IFNR and IL6R are both high for the single terminal state Maude reaches in this case (see previous subsection). If the search is expanded to include all states reachable by at least 1 rule execution, which includes the terminal state, and we require that IL4 is high and IGF1 is low, then there are many states (precisely 384, but this number is unimportant) in which either or both of IFNR and IL6R are high, but there are no states in which IFNR and IL6R are both low. This proves that Ab regulates the anti-inflammatory cytokines via autocrine interactions requiring IFNg or IL6 in the model. This interaction is a central feature of model behavior.

In the young case with Ab(1), ROS is always high (Table 2 Row 11), indicating that ROS is driven directly through the TLR complex. The same is not also true for phagocytosis. In the young case with

Ab(1), phago is not always but is eventually high (Table 2 Rows 12 and 13). In the model Smad is the dominant driver of phago, and like phago it is eventually high. Like IL4, Smad is not high until STAT1 is high (Table 2 Rows 14-16). STAT1 being high does not imply but does lead to phago being high (Table 2 Rows 17 and 18). In contrast, Smad being high does imply that phago is high (Table 2 Row 19). This analysis indicates that in the young case, Ab promotes phago largely through an autocrine interaction in which upregulation of pro-inflammatory cytokines such as IFNg or IL6 leads to JAK2 / STAT1 activation, which leads to generation of anti-inflammatory factors including TGFb, which leads to Smad activation, which increases phago. That Ab promotes phago largely through an autocrine mechanism involving STAT1 signaling is a central model feature (see below in this section).

These interactions account for the differences in model element levels in the young case for Ab(0) versus Ab(1) (Table 1 Rows 1 and 2). They also account for the differences in element levels in the young case for LPS(0) versus LPS(1) (Table 1 Rows 1 and 3), because LPS signals through the TLR complex just as Ab does in the model. The temporal-logic analysis just described illustrates how IFNg (or IL6) provides what could be called an "autocrine bridge" in the model by which an inflammatory response can lead to changes in expression (increases and decreases) of anti-inflammatory factors. An augmentation in the initial level of IFNg (i.e. IFNgini(8)) in the young case produces the same changes in cytokine levels and phagocytosis as does Ab(1) or LPS(1) in the model but does not increase ROS, because ROS is driven by TLR activation but that does not occur without Ab or LPS in the model (Table 1 Row 4). An augmentation in the initial level of IL4 (i.e. IL4ini(8)) in the young case has an entirely different outcome, which is analyzed in the next subsection.

**Response to IL4 augmentation in young condition**

An augmentation in the initial level of IL4 (i.e. IL4ini(8)) in the young case produces changes in model element levels that differ substantially from those produced by changes in the initial level of IFNg (Table 1 Rows 4, 5a, and 5b). Temporal-logic analysis of the model in the young case with IL4ini(8) is shown in Table 3. In this case, IL1b is not always low and IGF1 is not always high (Table 3 Row 1), indicating that the levels of these mediators change due to autocrine interactions in the model. Considered separately, IL1b is not always low and it is not even eventually low (Table 3 Rows 2 and 3). The latter is due to the existence of the two stable states associated with this case. From this we know that IL1b is eventually low for paths that lead to one stable state but not the other (Table 1 Rows 5a and 5b), so it is not true over all possible paths that IL1b is eventually low.

In contrast, IGF1 is not always high but it is eventually high (Table 3 Rows 4 and 5) and this means that IGF1 eventually attains the high level along all paths in the young case with IL4ini(8). IL4 signals through JAK2 and STAT6, and IL4ini(8) pushes STAT6 to a level above high, and STAT6 above high implies that IGF1 is high (Table 3 Row 6). Thus, IGF1 is driven high by the initially augmented level of IL4, but it does not always maintain that level because IGF1 being high does not imply that IGF1 remains high (Table 3 Row 7). Also, IGF1 needs to be high before IL1b is driven low, but IGF1 being high does not guarantee that IL1b eventually will be low (Table 3 Rows 7-9). The analysis so far indicates that, in the young case with IL4ini(8), the stable state in which IL1b is low and IGF1 is high depends on events that occur after the initial activation by IL4ini(8) of anti-inflammatory cytokines.

Temporal logic can be used to see which of the pro-inflammatory transcription factors must be decreased for IL1b to be driven low in the young case with IL4ini(8). These transcription factors are AP1, STAT3, and NFkB. All of these transcription factors are low in the stable state in which IL1b is low, and temporal logic proves that once they get low they stay low (Table 3 Rows 10-12). In other words, none of the pro-inflammatory transcription factors fall to the low level and then rise up again. It follows that if IL1b is low before a specific transcription factor is low, then that transcription factor could not be one that causes IL1b to get low. One way to check is to use the strong form of the logical implication operator to see which of the transcription factors are low whenever IL1b is low. The analysis shows that IL1b being low does not imply that AP1 is low or that STAT3 is low, but it does imply that NFkB is low (Table 3 Rows 13-15). This proves that NFkB is the transcription factor responsible for low expression of IL1b in the young case with IL4ini(8).

The foregoing has established that IL1b is not low until IGF1 is high (Table 3 Row 8), and that NFkB is the transcription factor that regulates IL1b in the young case with IL4ini(8). It remains to check the pathway from IL1b expression through NFkB and back to IGF1. The elements along this pathway are PPARg, PKC, and Gq (note that available data does not allow complete characterization of this pathway). In the stable state in which IL1b is low, NFkB is also low, PPARg and PKC are above high, and Gq is high. Temporal-logic analysis shows that none of these levels occur until IGF1 is high (Table 3 Rows 16-19). Although IGF1 being high does not necessarily lead to IL1b being low (Table 3 Row 9), Gq being high implies that IL1b is low (Table 3 Row 20). Similarly, IGF1 being high

does not necessarily lead to Gq being high, but Gq being high implies that IGF1 is high (Table 3 Rows 21 and 22). This seems circular but it is in fact explanatory.

If IGF1 brings Gq to the high level then Gq activates PKC. This leads to enhancement of PPARg, which enhances expression of anti-inflammatory factors including IGF1 itself but suppresses NFkB, which suppresses expression of pro-inflammatory factors. This leads to the "correct" stable state in which IL1b is low and IGF1 is high (Table 1 Row 5b). On the other hand, if IGF1 is brought back to base before it can bring Gq to the high level, then PPARg activity is not enhanced. Consequently expression of IGF1 is not enhanced and, for that reason, expression of pro-inflammatory factors is not suppressed. This leads to the stable state in which IL1b and IGF1 are both at the base level (Table 1 Row 5a). The abovementioned result that Gq being high implies that IGF1 is high (Table 3 Row 22) means that IGF1 is high whenever Gq is high. This in turn means that once IGF1 activates Gq it sustains its own activity because once Gq attains the high level it stays there (Table 3 Row 23).

This analysis provides insight into what is perhaps the most critical aspect of the model, which is that, in many cases including those with Ab(1), expression of pro- and anti-inflammatory factors are increased together except for IGF1, expression of which is decreased (Table 1). Importantly, in those cases in which expression of IGF1 is increased, expression of anti-inflammatory factors is also increased but expression of pro-inflammatory factors is decreased (Table 1). These are the cases with the most compelling therapeutic potential and suggest a critical role for IGF1 signaling (see below).

The analysis in the previous subsection shows that IFNg is an autocrine bridge over which a pro-inflammatory trigger such as Ab(1) can also upregulate anti-inflammatory factors. The analysis in this subsection shows that IGF1 is the autocrine bridge over which an overwhelming anti-inflammatory trigger such as IL4ini(8) can downregulate pro-inflammatory factors. Of the two bridges IGF1 is the more precarious. IFNg can be maintained at the high level through autocrine feedback involving itself and IL1b, IL6, and TNFa, which signal through AP1 and STAT3. In contrast, once brought to the high level by initially augmented IL4ini(8) and STAT6, IGF1 must maintain itself over its pathway from Gq to PKC to PPARg. If it fails to do so, the therapeutically favorable state in which IGF1 and the other anti-inflammatory factors and phagocytosis are high, but ROS and pro-inflammatory factors are low (Table 1), does not occur. Pharmacological enhancement of PPARγ has already been shown to move microglia in the direction of this therapeutically favorable state. The model suggests PKC as another therapeutically advantageous target (see below).

**Response to Aβ and LPS in the old condition**

What distinguishes the old from the young condition in the model is the absence of ACh and the neuronal surface ligands CD22, CD200, CX3CL1, and TREM2L. The ligand CD40L remains. This reflects a pattern expected in old brains in which neurons, especially cholinergic neurons, are dying, and because CD22, CD200, CX3CL1, and TREM2L are expressed by healthy neurons while CD40L is expressed by necrotic neurons. The effects of these neuronal factors vary but CD22, CD200, CX3CL1, and TREM2L are generally anti-inflammatory while CD40L is pro-inflammatory. In the model the net effect of the loss of CD22, CD200, CX3CL1, and TREM2L is upregulation of pro-inflammatory cytokines, which leads to upregulation of anti-inflammatory cytokines (Table 1 Row 6). The latter occurs by crossing the IFNg autocrine bridge as described in the young case in the presence of Ab (see above) but in the old case it also occurs in the absence of Ab. Temporal logic analysis reveals the basis of the similarities and differences between these two cases.

In the young case with Ab(1), NFkB is always high (Table 2 Row 2) because it is set by Ab through the TLR complex (see above). The resulting upregulation of IFNg and IL6 then leads to upregulation of the anti-inflammatory cytokines except for IGF1. In contrast, NFkB is not always high in the old case with Ab(0) but NFkB is eventually high (Table 4 Rows 1 and 2), indicating that NFkB is driven up by autocrine feedback in the model. Similarly, STAT3 is not always high but is eventually high (Table 4 Rows 3 and 4). The only other transcription factor in the model that could initiate upregulation of the pro-inflammatory cytokines is AP1, and analysis shows that AP1 is always greater than base in the old case without Ab or LPS (Table 4 Row 5). Thus, AP1 is the transcription factor responsible for pro-inflammatory upregulation in this case.

In the model, AP1 is driven by p38MAPK and JNK (specifically, AP1 takes whichever of the p38MAPK or JNK levels that is greater), and p38MAPK and JNK are similarly always greater than base (Table 4 Rows 6 and 7). The picture that emerges in the old case is that the absence of CD22, CD200, CX3CL1, and TREM2L pushes p38MAPK and JNK above base, which pushes AP1 above base, and this brings the pro-inflammatory cytokines up to the high level of expression without autocrine feedback since IL1b and IFNg are both always high (Table 4 Rows 8 and 9). However, autocrine feedback subsequently pushes p38MAPK, JNK, and AP1 to the high level and slightly above. Again activation of

IFNg (or IL6) acts as an autocrine bridge to upregulate the anti-inflammatory cytokines, as it does in the young case with Ab(1), and this accounts for the pattern of expression in the old case.

The output patterns in the young case with Ab(1) and in the old case with Ab(0) are the same with two exceptions (Table 1 Rows 2 and 6). The first exception is that ROS is high in the young Ab(1) case but at base in the old Ab(0) case. This difference is easy to explain because ROS is driven by the TLR complex in the model, which is in turn activated by Ab or LPS, neither of which are present in the unstimulated, old case being analyzed here. The second exception is that phago is high in the young Ab(1) case but low in the old Ab(0) case. This situation persists in the old case even when Ab and/or LPS are present (Table 1 Rows 6-9), as it must do in order to agree with observation. The interactions that govern phago in the model are set to reproduce these observations based on specific patterns of activity of the elements that determine the level of phago but are not critical model features in themselves.

Experiments show that microglia from aged specimens are inflammatory even without Aβ or LPS as stimuli. The model reflects this (Table 1 Row 6) and it follows, due to the IFNg autocrine bridge, that old microglia should produce some anti-inflammatory factors along with the pro-inflammatory cytokines (see below). In the presence either of Ab or LPS in the model, the old output pattern is the same as it is without Ab or LPS, except that ROS is high (Table 1 Rows 7 and 8). This result, as described in the previous paragraph, is due to activation of the TLR complex by Ab or LPS.

The output pattern in the old case changes dramatically when Ab and LPS are combined. In the old case with Ab(1) *and* LPS(1), the pro-inflammatory cytokines IL1b and TNFa remain high, ROS is high, and phago is low, but all the anti-inflammatory factors are driven low. Temporal-logic analysis reveals the basis of this effect. In the old case with Ab(1) and LPS(1), IL1b and IFNg are always high and IL4 is always low (Table 5 Rows 1-3), indicating that these pro- and anti-inflammatory cytokine levels do not depend on autocrine feedback in this case. In contrast, IGF1 is not always low but it is eventually low (Table 5 Rows 2-4), indicating that the IGF1 level does depend on autocrine interactions in this case. Further analysis reveals the transcription factors responsible for these effects.

NFκB can be driven via TAK1 either by pro-inflammatory cytokines or by activation of the TLR complex. In the old case, synergistic activation of the TLR complex by Ab(1) and LPS(1) drives NFkB above high by the TLR complex, and this pushes IL1b and IFNg up to the high level (Table 5 Rows 5 and 6). This level of NFkB activation also drives PPARg to the low level, and that pushes IL4 to

the low level but does not do the same for IGF1 (Table 5 Rows 7-10). With RXR and LXRb at constitutive levels, as they are in this case, the only other transcription factors that could reduce the IGF1 level are STAT1 and STAT6. STAT1 is not always but is eventually high while STAT6 is not always but is eventually low (Table 5 Rows 11-14), indicating that the levels of both factors depend on autocrine interactions in the model. Further analysis shows that IGF1 can reach the low level before STAT6 reaches its low level, but IGF1 cannot reach the low level before STAT1 reaches the high level (Table 5 Rows 15 and 16). These results proves that STAT1 is the transcription factor responsible for driving down IGF1 in the model in the old case with Ab(1) and LPS(1).

The transcription factor STAT1 is activated by JAK2 following binding of IFNγ or IL6 to their receptors. In the model in the old case with Ab(1) and LPS(1), STAT1 is not high until either IFNg or IL6 is high and, given the dependence of IGF1 on STAT1 in this case, it is not surprising that IGF1 is not low until IFNg or IL6 are high (Table 5 Rows 17 and 18). These results together show that, in the old case with Ab(1) and LPS(1), IGF1 is driven low over the IFNg autocrine bridge (and IL6 can serve the same bridging function, see next subsection). The reason why the IFNg autocrine bridge does not also activate the other anti-inflammatory cytokines in the old case with Ab(1) and LPS(1), as it does in the young case with either Ab(1) or LPS(1), is that the signal due to STAT1 is overridden by PPARg at the low level (Table 5 Row 9). This state, in which all of the pro-inflammatory cytokines are expressed at a high level while all of the anti-inflammatory factors are expressed at a low level, and in which ROS is high but phagocytosis is low, is observed experimentally in old microglia *in vitro* when the TLR complex is synergistically stimulated by Aβ and LPS. This microglial phenotype has not been described as part of AD pathogenesis *in vivo* but obviously it would be devastating if it did occur. Because it can be seen as a hyperinflammatory phenotype it is of interest to see how it could be reversed in the model.

**Reversing inflammatory microglial phenotypes**

In cultures of microglia from aged animals, a hyperinflammatory phenotype due to the synergistic interaction of Aβ and LPS can be mitigated with an augmentation in the level of IL4. The same occurs in the model but, as in the young case, the model in the old case with Ab(1) and LPS(1) has two stable states with IL4ini(8) as an initial condition (Table 1 Rows 5a, 5b, 10a, and 10b). In one of the states reachable from IL4ini(8) in the old case with Ab(1) and LPS(1), the neurotoxicity is just as extreme as it is without IL4ini(8), but in the other state it is reversed except that ROS is not driven low but returns to base (Table 1 Rows 10a and 10b). The mechanisms responsible for this reversal are

similar to those described in the young case with IL4ini(8) (Table 3), and the analysis developed in that case (see above) can be abbreviated and re-ordered for this case (Table 6).

As in the young case with IL4ini(8), the augmented initial IL4 level drives STAT6 above high and this pushes IGF1 to the high level (Table 6 Row 1). Again as in the young case, if IGF1 then activates Gq before the initially augmented level of IL4 subsides, then IGF1 will sustain itself by driving PKC above high, which will drive PPARg above high, and PPARg will keep IGF1 at the high level (Table 6 Rows 2-5). The actual analysis proceeds backward from establishment of the fact that IGF1 is activated by STAT6 above high and once that occurs IGF1 stays high if it activates the pathway from Gq to PKC to PPARg.

As in the young case with IL4ini(8), PPARg above high drives NFkB to the low level and this brings IL1b (Table 6 Rows 6 and 7) and the other pro-inflammatory cytokines to the low level also. In contrast, PPARg above high drives IL10 (Table 6 Row 8) and the other anti-inflammatory cytokines (including IGF1) to the high level. ROS is initially brought high through activation of the TLR complex by Ab(1) and LPS(1) but it is brought back to base after IGF1 reaches the high level (Table 6 Row 9) and suppresses ROS over the PI3K pathway. PPARg above high also drives TGFb high and TGFb then activates phago via Smad (Table 6 Rows 10-12). In this way the initially augmented level of IL4 reverses what would be a highly neurotoxic model state into a highly neuroprotective model state. The reversal begins with initial upregulation of IGF1 by IL4 but its consummation hinges on subsequent activation of Gq by IGF1, so the achievement of this neuroprotective state is somewhat precarious. The model offers more direct alternatives.

Experiments show that IGF1 reduces ROS and TNFα production by inflammatory microglia, suggesting that application of IGF1 itself may be a more direct way to achieve the highly neuroprotective state. The model with IGF1ini(8) is consistent with this suggestion (Table 1 Row 11). The biological experiments were conducted in the absence of stimulation of the TLR complex and perhaps for that reason IGF1 is able to decrease ROS below its baseline; the same occurs in the model (see Table 1 Row 11). Temporal logic analysis of the model shows that this effect is due to initial and sustained activation of Gq since Gq is always at or above high with IGF1ini(8).

Experiments also show that augmentation of PPARγ signaling using either rosiglitazone or retinoic acid can decrease expression of pro-inflammatory cytokines, increase expression of anti-inflammatory

cytokines, and enhance phagocytosis of Aβ in old microglia even after stimulation by TLR2/4 ligands. The model reproduces these general findings (Table 1 Rows 12 and 13). Temporal logic analysis of the model in the old case with Ab(1) shows that Gq is eventually high and once high stays high either with rosi(1) or retino(1). These results show that rosi or retino, or IGF1 itself, can activate the Gq pathway and lead to a sustained, neuroprotective state, and they all do so more directly and reliably than Il4. These results suggest that activation of this pathway, which drives the microglia system over the IGF1 autocrine bridge, could be an effective means of pushing inflamed microglia toward a more neuroprotective phenotype.

**Main themes and predictions emerging from the model**

The main themes that emerge from the model are the potential autocrine bridges involving IFNg and IGF1. The main predictions from the model focus on these two mechanisms. Experimental data is overwhelmingly consistent with the general finding that activation of the TLR complex by Aβ leads to increased microglial production of anti-inflammatory as well as pro-inflammatory cytokines. The model suggests that this occurs over an autocrine bridge by which initial upregulation of IFNg (or IL6), along with other pro-inflammatory cytokines, leads via JAK2 and STAT1 to upregulation of IL4, IL10, TGFb, and other anti-inflammatory factors (but downregulation of IGF1; see above). The model predicts that disruption of JAK2 / STAT1 signaling should severely dysregulate this mechanism.

In the model STAT1 is a key player and its removal has complex effects. Removal of STAT1 prevents induction by Ab of the upregulation of Ym1, IL4, IL10, and TGFb that occurs in the model in the young case when STAT1 is present (Table 1 Rows 1 and 2; Table 2 Rows 3-10). Without STAT1, all of these anti-inflammatory factors stay at baseline, indicating that the autocrine bridge by which Ab upregulates anti-inflammatory factors has been disrupted. Removal of STAT1 also prevents the increase in phago due to Ab that occurs in the model in the young case when STAT1 is present (Table 1 Rows 1 and 2; Table 2 Rows 12-19). In contrast, STAT1 is instrumental in the induction by Ab of downregulation of IGF1 that occurs in the young case when STAT1 is present (Table 1 Rows 1 and 2; Table 2 Rows 3-10), and removal of STAT1 in the young case in the model actually results in upregulation by Ab of IGF1. Because upregulation of IGF1 results in downregulation of IL1b and other pro-inflammatory cytokines (Table 3 Rows 16-20), Ab actually causes downregulation of pro-inflammatory cytokines in the young case when STAT1 is removed. Thus, the model predicts that exposure to Aβ of young microglia that lack STAT1 should increase production of IGF1 but not of other anti-inflammatory factors, should not

increase phagocytosis, and should actually decrease production of pro-inflammatory cytokines, secondary to the increase in IGF1.

Experimental data are also consistent with the general finding that microglia convert to a pro-inflammatory phenotype with age and maintain that phenotype. The model suggests that old microglia could be pushed toward a more neuroprotective phenotype through activation of a pathway from IGF2R through Gq, PKC, and PPARg, but that indirect activation of this pathway by upregulation of IGF1 by IL4 may be unreliable (see above). This could explain why old microglia tend to remain in a pro-inflammatory state. Experimental findings show that augmentation of PPARγ can induce a more neuroprotective phenotype including increased Aβ phagocytosis, and the model is consistent with these general findings (see above). The model suggests that PKC would also play a critical role in the conversion of the pro-inflammatory phenotype in old microglia to a more neuroprotective state. In the model the effects of removal of PKC are straightforward.

In the model in the old case, the levels of the factors ACh, CD22, CD200, CX3CL1, and TREM2L are switched from 1 to 0, which concisely reflects their reduction with age. In the model in the old case, a hyperinflammatory state, characterized by high and low levels of pro- and anti-inflammatory factors, respectively, and by high ROS but low phago, is brought about by the synergistically inflammatory combination of Ab and LPS (Table 1 Row 9). The level of LPS, a pro-inflammatory stimulus derived from the outer membranes of Gram-negative bacteria, could build up with age due to repeated bacterial infections [1b]. The hyperinflammatory phenotype has not been observed *in vivo*, but something similar to it is plausible in the aged and AD brain due to the possible confluence of low ACh, CD22, CD200, CX3CL1, and TREM2L and high Aβ and LPS. In the model, this hyperinflammatory phenotype is almost completely reversed by augmented initial IGF1, which brings pro-inflammatory cytokines low, anti-inflammatory factors high, and also brings phago high. The exception to complete reversal is that ROS is not brought low but is returned to base (see above). The straightforward effect of removal of PKC in the model is to completely block the effects of augmented initial IGF1.

In the model, augmented initial IGF1 also reduces pro-inflammatory cytokines in the old case when Ab and LPS are both absent (Table 1 Rows 6 and 11), and this is consistent with observation. Removal of PKC in the model in the old case completely blocks this reduction in pro-inflammatory cytokines. These modeling results point to two model predictions. First, the model posits a hyperinflammatory microglial phenotype in the aged and AD brain that could be reversed by augmented IGF1, but this reversal should

depend on PKC. Second, and more generally, the model predicts that any reduction in inflammation due to augmented IGF1 should not occur in the absence of PKC.

These predictions on STAT1 and PKC address the most critical features of the model, but any model result could be considered a model prediction. For example, on the output side of the truth table (Table 1), any plain numeral can be considered as a prediction of the model concerning an increase, decrease, or no change (respectively 7, 3, or 5) in a factor given the corresponding input conditions on the input side of the truth table. One potentially interesting truth-table prediction concerns microglia from aging brains. Studies of microglia and aging generally do not measure levels of anti-inflammatory cytokines, but the model suggests increased microglial production of IL4, IL10, and other anti-inflammatory cytokines along with the observed increase in production of pro-inflammatory cytokines such as IL1β and TNFα. The truth table modeling results also suggest that expression of most anti-inflammatory mediators should be increased whenever expression of IGF1 is increased.

**Some questions raised in the modeling process**

Aside from adding perspective and making predictions, a model can be useful in identifying pieces missing from the puzzle it strives to fit together. Several missing pieces were identified in the process of specifying the microglia signaling system model. One concerns the mutually antagonistic relationship between PPARγ and NFκB that has been uncovered in macrophages [61]. This interaction is a critical feature of the microglia signaling model because it allows IGF1 to suppress production of pro-inflammatory cytokines and to reverse neurotoxic phenotypes. The model predicts that such a mutually antagonistic relationship between PPARγ and NFκB should also exist in microglia.

Some of the findings on neuronal membrane-bound or secreted factors are confusing in the context of the model. Some concern fractalkine, which seems consistently to suppress phagocytosis and decrease expression of some pro-inflammatory cytokines but to increase expression of others. How fractalkine signaling can accomplish such cytokine fine tuning is at present unclear. Similarly, activation of TREM2 by TREM2L has been found to reduce the expression of pro-inflammatory cytokines, but TREM2 signals via DAP12, which activates Syk. Confusingly, Aβ activates the TLR complex and that also activates Syk, and this leads to ROS production but not to reduction in expression of pro-inflammatory cytokines. Given the signaling pathways as described so far in the literature and as represented in the model, it is not clear how TREM2 activation could lead to suppression of pro-inflammatory cytokine production.

TREM2 activation has also been shown to promote microglial phagocytosis. In the model, both TREM2 and the TLR complex promote phagocytosis by activating GRB2 which activates ERK (Figure 1). In order that TREM2 could promote phago but not promote expression of pro-inflammatory cytokines in the model, ERK was not coupled to AP1. Apparently, ERK does activate AP1 in some cells [85], but the model suggests ERK does not activate AP1 in microglia. TREM2 has recently emerged as an important player in AD pathogenesis. Further exploration of ERK signaling in microglia could help elucidate the important rule of TREM2 in the AD/inflammatory connection.

## Conclusions

Few computational models of the microglial component of AD have appeared. A recent model represents some of the interactions between microglia, astroglia, and neurons that are relevant to Aβ toxicity, and supports the idea that microglia are central to AD neurodegeneration [86]. That model is based on differential rate equations and, perforce, makes quantitative assumptions concerning rate parameters. It is different in kind from the microglia signaling model presented here, which is based directly on experimental data and represents signaling interactions in a course-grained fashion that is consistent with the qualitative terms in which the data are described in the literature. The new approach taken here is to use specialized computational techniques to analyze rigorously a system model that a modeler specifies by directly fitting together a large set of individual facts. The model provides a new, high-level view that helps to organize findings and suggest avenues for further research.

The microglia signaling model represents much of what is currently known concerning the effects on microglia of Aβ, but it is still very far from a complete characterization of microglia. The most immediate direction for continued development of the model is to include more of what is known about microglial signaling. Concerning the inflammatory contribution to AD, an important area for further development is to model inflammatory influences on Aβ metabolism. The current model treats Aβ purely as an input, not as an element that is itself dependent on interactions with other model elements. In fact, while Aβ can activate microglia, the inflammatory response due to microglia can also increase Aβ production [1c]. This can occur in at least two ways. First, IL1β can upregulate amyloid precursor protein (APP) [87], which is the protein from which Aβ is derived [3]. Second, PPARγ can downregulate β-secretase (BACE) [55], one of the two enzymes responsible for the proteolytic processing that produces Aβ from APP [3]. By downregulating PPARγ, IL1β and other inflammatory cytokines upregulate BACE. Thus, inflammatory cytokines increase Aβ by

upregulating both BACE and its substrate, APP. Maude-based models of Aβ metabolism already exist [25a, b]. By joining these models with the microglia system model, future modeling efforts can close the loop and represent the mutually reinforcing but pathological interaction between Aβ production and inflammation.

The most critical direction for future development is to couple modeling with experimentation. Because it directly represents experimental findings, model predictions can be tested using the same techniques that were used to generate the data on which the model is based. Using such test results the model can be confirmed or corrected and expanded, new predictions can be generated, and the cycle can be continued, producing a model of ever increasing explanatory power. The main purpose of the modeling described here is to initiate such a computational/experimental interaction.

## References


1. (a) H. Johnston, H. Boutin, S. M. Allan, Assessing the contribution of inflammation in models of Alzheimer's disease. *Biochemical Society transactions* 2011, *39*. 886-90, DOI: 10.1042/BST0390886; (b) J. Miklossy, Chronic inflammation and amyloidogenesis in Alzheimer's disease -- role of Spirochetes. *Journal of Alzheimer's disease : JAD* 2008, *13*. 381-91; (c) R. von Bernhardi, Glial cell dysregulation: a new perspective on Alzheimer disease. *Neurotoxicity research* 2007, *12*. 215-32; (d) A. Piazza, M. A. Lynch, Neuroinflammatory changes increase the impact of stressors on neuronal function. *Biochemical Society transactions* 2009, *37*. 303-7, DOI: 10.1042/BST0370303; (e) W. S. Griffin, R. E. Mrak, Interleukin-1 in the genesis and progression of and risk for development of neuronal degeneration in Alzheimer's disease. *Journal of leukocyte biology* 2002, *72*. 233-8; (f) S. Mandrekar-Colucci, G. E. Landreth, Microglia and inflammation in Alzheimer's disease. *CNS & neurological disorders drug targets* 2010, *9*. 156-67.
2. C. L. Masters, G. Simms, N. A. Weinman, G. Multhaup, B. L. McDonald, K. Beyreuther, Amyloid plaque core protein in Alzheimer disease and Down syndrome. *Proceedings of the National Academy of Sciences of the United States of America* 1985, *82*. 4245-9.
3. J. Hardy, D. J. Selkoe, The amyloid hypothesis of Alzheimer's disease: progress and problems on the road to therapeutics. *Science* 2002, *297*. 353-6, DOI: 10.1126/science.1072994.
4. (a) B. Cameron, G. E. Landreth, Inflammation, microglia, and Alzheimer's disease. *Neurobiol Dis* 2010, *37*. 503-9, DOI: 10.1016/j.nbd.2009.10.006; (b) J. J. Bajramovic, Regulation of innate immune responses in the central nervous system. *CNS & neurological disorders drug targets* 2011, *10*. 4-24.
5. C. Schwab, A. Klegeris, P. L. McGeer, Inflammation in transgenic mouse models of neurodegenerative disorders. *Biochimica et biophysica acta* 2010, *1802*. 889-902, DOI: 10.1016/j.bbadis.2009.10.013.
6. (a) P. L. McGeer, M. Schulzer, E. G. McGeer, Arthritis and anti-inflammatory agents as possible protective factors for Alzheimer's disease: a review of 17 epidemiologic studies. *Neurology* 1996, *47*. 425-32; (b) W. F. Stewart, C. Kawas, M. Corrada, E. J. Metter, Risk of Alzheimer's disease and duration of NSAID use. *Neurology* 1997, *48*. 626-32; (c) J. C. Anthony, J. C. Breitner, P. P. Zandi, M. R. Meyer, I. Jurasova, M. C. Norton, S. V. Stone, Reduced prevalence of AD in users of NSAIDs and H2 receptor antagonists: the Cache County study. *Neurology* 2000, *54*. 2066-71; (d) B. A. in t' Veld, A. Ruitenberg, A. Hofman, L. J. Launer, C. M. van Duijn, T. Stijnen, M. M. Breteler, B. H. Stricker, Nonsteroidal antiinflammatory drugs and the risk of Alzheimer's disease. *The New England journal of medicine* 2001, *345*. 1515-21, DOI: 10.1056/NEJMoa010178.
7. (a) I. R. Mackenzie, D. G. Munoz, Nonsteroidal anti-inflammatory drug use and Alzheimer-type pathology in aging. *Neurology* 1998, *50*. 986-90; (b) I. Alafuzoff, M. Overmyer, S. Helisalmi, H. Soininen, Lower Counts of Astroglia and Activated Microglia in Patients with Alzheimer's Disease with Regular Use of Non-Steroidal Anti-Inflammatory Drugs. *Journal of Alzheimer's disease : JAD* 2000, *2*. 37-46.
8. (a) G. P. Lim, F. Yang, T. Chu, P. Chen, W. Beech, B. Teter, T. Tran, O. Ubeda, K. H. Ashe, S. A. Frautschy, G. M. Cole, Ibuprofen suppresses plaque pathology and inflammation in a mouse model for Alzheimer's disease. *The Journal of neuroscience : the official journal of the Society for Neuroscience* 2000, *20*. 5709-14; (b) Q. Yan, J. Zhang, H. Liu, S. Babu-Khan, R. Vassar, A. L. Biere, M. Citron, G. Landreth, Anti-inflammatory drug therapy alters beta-amyloid processing and deposition in an animal model of Alzheimer's disease. *The Journal of neuroscience : the official journal of the Society for Neuroscience* 2003, *23*. 7504-9; (c) S. Sung, H. Yang, K. Uryu, E. B. Lee, L. Zhao, D. Shineman, J. Q. Trojanowski, V. M. Lee, D. Pratico, Modulation of nuclear factor-kappa B activity by indomethacin influences A beta levels but not A beta precursor protein metabolism in a model of Alzheimer's disease. *The American journal of pathology* 2004, *165*. 2197-206.

9. M. Q. Xia, B. T. Hyman, Chemokines/chemokine receptors in the central nervous system and Alzheimer's disease. *Journal of neurovirology* 1999, *5*. 32-41, DOI: 10.3109/13550289909029743.
10. A. R. Simard, D. Soulet, G. Gowing, J. P. Julien, S. Rivest, Bone marrow-derived microglia play a critical role in restricting senile plaque formation in Alzheimer's disease. *Neuron* 2006, *49*. 489-502, DOI: 10.1016/j.neuron.2006.01.022.
11. A. Serrano-Pozo, T. Gomez-Isla, J. H. Growdon, M. P. Frosch, B. T. Hyman, A phenotypic change but not proliferation underlies glial responses in Alzheimer disease. *The American journal of pathology* 2013, *182*. 2332-44, DOI: 10.1016/j.ajpath.2013.02.031.
12. S. Jimenez, D. Baglietto-Vargas, C. Caballero, I. Moreno-Gonzalez, M. Torres, R. Sanchez-Varo, D. Ruano, M. Vizuete, A. Gutierrez, J. Vitorica, Inflammatory response in the hippocampus of PS1M146L/APP751SL mouse model of Alzheimer's disease: age-dependent switch in the microglial phenotype from alternative to classic. *The Journal of neuroscience : the official journal of the Society for Neuroscience* 2008, *28*. 11650-61, DOI: 10.1523/JNEUROSCI.3024-08.2008.
13. V. Vasilevko, D. H. Cribbs, Novel approaches for immunotherapeutic intervention in Alzheimer's disease. *Neurochemistry international* 2006, *49*. 113-26, DOI: 10.1016/j.neuint.2006.03.019.
14. C. Li, R. Zhao, K. Gao, Z. Wei, M. Y. Yin, L. T. Lau, D. Chui, A. C. Hoi Yu, Astrocytes: implications for neuroinflammatory pathogenesis of Alzheimer's disease. *Current Alzheimer research* 2011, *8*. 67-80.
15. J. F. Monin, M. G. Hinchey, *Understanding Formal Methods*. Springer Verlag: London, 2003.
16. M. Huth, M. Ryan, *Logic in Computer Science: Modelling and Reasoning about Systems*. 2 ed.; Cambridge University Press: Cambridge, 2004.
17. (a) S. A. Kauffman, Metabolic stability and epigenesis in randomly constructed genetic nets. *Jouranl of Theoretical Biology* 1969, *22*. 437-467, DOI: 10.1016/0022-5193(69)90015-0; (b) R. Thomas, Boolean formalization of genetic control circuits. *Jouranl of Theoretical Biology* 1973, *42*. 563-585, DOI: 10.1016/0022-5193(73)90247-6; (c) L. Glass, S. A. Kauffman, The logical analysis of continuous, non-linear biochemical control networks. *Journal of theoretical biology* 1973, *39*. 103-29; (d) L. Glass, Classification of biological networks by their qualitative dynamics. *Jouranl of Theoretical Biology* 1975, *54*. 85-107, DOI: 10.1016/S0022-5193(75)80056-7.
18. (a) S. Klamt, J. Saez-Rodriguez, J. A. Lindquist, L. Simeoni, E. D. Gilles, A methodology for the structural and functional analysis of signaling and regulatory networks. *BMC bioinformatics* 2006, *7*. 56, DOI: 10.1186/1471-2105-7-56; (b) S. Klamt, J. Saez-Rodriguez, E. D. Gilles, Structural and functional analysis of cellular networks with CellNetAnalyzer. *BMC systems biology* 2007, *1*. 2, DOI: 10.1186/1752-0509-1-2; (c) J. Saez-Rodriguez, L. G. Alexopoulos, J. Epperlein, R. Samaga, D. A. Lauffenburger, S. Klamt, P. K. Sorger, Discrete logic modelling as a means to link protein signalling networks with functional analysis of mammalian signal transduction. *Molecular systems biology* 2009, *5*. 331, DOI: 10.1038/msb.2009.87.
19. (a) R. Franke, F. J. Theis, S. Klamt, From binary to multivalued to continuous models: the lac operon as a case study. *Journal of integrative bioinformatics* 2010, *7*. DOI: 10.2390/biecoll-jib-2010-151; (b) F. Liu, M. A. Blatke, M. Heiner, M. Yang, Modelling and simulating reaction-diffusion systems using coloured Petri nets. *Computers in biology and medicine* 2014. DOI: 10.1016/j.compbiomed.2014.07.004; (c) M. Durzinsky, A. Wagler, W. Marwan, Reconstruction of extended Petri nets from time series data and its application to signal transduction and to gene regulatory networks. *BMC systems biology* 2011, *5*. 113, DOI: 10.1186/1752-0509-5-113.
20. J. Fisher, T. A. Henzinger, Executable cell biology. *Nature biotechnology* 2007, *25*. 1239-49, DOI: 10.1038/nbt1356.

21. (a) M. L. Wynn, N. Consul, S. D. Merajver, S. Schnell, Logic-based models in systems biology: a predictive and parameter-free network analysis method. *Integrative biology : quantitative biosciences from nano to macro* 2012, *4*. 1323-37, DOI: 10.1039/c2ib20193c; (b) R. Samaga, S. Klamt, Modeling approaches for qualitative and semi-quantitative analysis of cellular signaling networks. *Cell communication and signaling : CCS* 2013, *11*. 43, DOI: 10.1186/1478-811X-11-43.
22. M. Clavel, R. Durán, S. Eker, P. Lincoln, N. Martí-Oliet, J. Meseguer, C. Talcott, *All About Maude – A High-Preformance Logical Framework: How to Specify, Program, and Verify Systems in Rewriting Logic*. Springer: Berlin, 2007; Vol. 4350.
23. J. Meseguer, Twenty years of rewriting logic. *The Journal of Logic and Algebraic Programming* 2012.
24. (a) S. Eker, M. Knapp, K. Laderoute, P. Lincoln, J. Meseguer, K. Sonmez, Pathway logic: symbolic analysis of biological signaling. *Pacific Symposium on Biocomputing. Pacific Symposium on Biocomputing* 2002. 400-12; (b) C. Talcott, in *Lecture Notes in Computer Science*, ed. M. Bernardo, P. Degano, G. Zavattaro. Springer: Berlin, 2008, vol. 5016, pp 21-53.
25. (a) T. J. Anastasio, Data-driven modeling of Alzheimer disease pathogenesis. *Journal of theoretical biology* 2011, *290*. 60-72, DOI: 10.1016/j.jtbi.2011.08.038; (b) T. J. Anastasio, Exploring the contribution of estrogen to amyloid-Beta regulation: a novel multifactorial computational modeling approach. *Frontiers in pharmacology* 2013, *4*. 16, DOI: 10.3389/fphar.2013.00016; (c) T. J. Anastasio, Computational identification of potential multitarget treatments for ameliorating the adverse effects of amyloid-beta on synaptic plasticity. *Frontiers in pharmacology* 2014.
26. M. Di Carlo, Beta amyloid peptide: from different aggregation forms to the activation of different biochemical pathways. *European biophysics journal : EBJ* 2010, *39*. 877-88, DOI: 10.1007/s00249-009-0439-8.
27. (a) M. E. Bamberger, M. E. Harris, D. R. McDonald, J. Husemann, G. E. Landreth, A cell surface receptor complex for fibrillar beta-amyloid mediates microglial activation. *The Journal of neuroscience : the official journal of the Society for Neuroscience* 2003, *23*. 2665-74; (b) E. G. Reed-Geaghan, J. C. Savage, A. G. Hise, G. E. Landreth, CD14 and toll-like receptors 2 and 4 are required for fibrillar A{beta}-stimulated microglial activation. *The Journal of neuroscience : the official journal of the Society for Neuroscience* 2009, *29*. 11982-92, DOI: 10.1523/JNEUROSCI.3158-09.2009; (c) J. Koenigsknecht, G. Landreth, Microglial phagocytosis of fibrillar beta-amyloid through a beta1 integrin-dependent mechanism. *The Journal of neuroscience : the official journal of the Society for Neuroscience* 2004, *24*. 9838-46, DOI: 10.1523/JNEUROSCI.2557-04.2004; (d) M. L. D. Udan, D. Ajit, N. R. Crouse, M. R. Nichols, Toll-like receptors 2 and 4 mediate Abeta(1-42) activation of the innate immune response in a human monocytic cell line. *Journal of Neurochemistry* 2008, *104*. 524-533, DOI: 17986235.
28. (a) D. R. McDonald, K. R. Brunden, G. E. Landreth, Amyloid fibrils activate tyrosine kinase-dependent signaling and superoxide production in microglia. *The Journal of neuroscience : the official journal of the Society for Neuroscience* 1997, *17*. 2284-94; (b) C. K. Combs, D. E. Johnson, S. B. Cannady, T. M. Lehman, G. E. Landreth, Identification of microglial signal transduction pathways mediating a neurotoxic response to amyloidogenic fragments of beta-amyloid and prion proteins. *The Journal of neuroscience : the official journal of the Society for Neuroscience* 1999, *19*. 928-39.
29. B. Wilkinson, J. Koenigsknecht-Talboo, C. Grommes, C. Y. Lee, G. Landreth, Fibrillar beta-amyloid-stimulated intracellular signaling cascades require Vav for induction of respiratory burst and phagocytosis in monocytes and microglia. *J Biol Chem* 2006, *281*. 20842-50, DOI: 10.1074/jbc.M600627200.
30. V. D. Bianca, S. Dusi, E. Bianchini, I. Dal Pra, F. Rossi, beta-amyloid activates the O-2 forming NADPH oxidase in microglia, monocytes, and neutrophils. A possible inflammatory mechanism of neuronal damage in Alzheimer's disease. *J Biol Chem* 1999, *274*. 15493-9.

31. K. M. Park, W. J. Bowers, Tumor necrosis factor-alpha mediated signaling in neuronal homeostasis and dysfunction. *Cellular signalling* 2010, *22*. 977-83, DOI: 10.1016/j.cellsig.2010.01.010.
32. (a) J. J. Jin, H. D. Kim, J. A. Maxwell, L. Li, K. Fukuchi, Toll-like receptor 4-dependent upregulation of cytokines in a transgenic mouse model of Alzheimer's disease. *Journal of neuroinflammation* 2008, *5*. 23, DOI: 10.1186/1742-2094-5-23; (b) K. L. Richard, M. Filali, P. Prefontaine, S. Rivest, Toll-like receptor 2 acts as a natural innate immune receptor to clear amyloid beta 1-42 and delay the cognitive decline in a mouse model of Alzheimer's disease. *The Journal of neuroscience : the official journal of the Society for Neuroscience* 2008, *28*. 5784-93, DOI: 10.1523/JNEUROSCI.1146-08.2008; (c) M. Song, J. Jin, J. E. Lim, J. Kou, A. Pattanayak, J. A. Rehman, H. D. Kim, K. Tahara, R. Lalonde, K. Fukuchi, TLR4 mutation reduces microglial activation, increases Abeta deposits and exacerbates cognitive deficits in a mouse model of Alzheimer's disease. *Journal of neuroinflammation* 2011, *8*. 92, DOI: 10.1186/1742-2094-8-92.
33. S. Dennler, M. J. Goumans, P. ten Dijke, Transforming growth factor beta signal transduction. *Journal of leukocyte biology* 2002, *71*. 731-40.
34. T. Wyss-Coray, C. Lin, F. Yan, G. Q. Yu, M. Rohde, L. McConlogue, E. Masliah, L. Mucke, TGF-beta1 promotes microglial amyloid-beta clearance and reduces plaque burden in transgenic mice. *Nat Med* 2001, *7*. 612-8, DOI: 10.1038/87945.
35. S. S. Shaftel, S. Kyrkanides, J. A. Olschowka, J. N. Miller, R. E. Johnson, M. K. O'Banion, Sustained hippocampal IL-1 beta overexpression mediates chronic neuroinflammation and ameliorates Alzheimer plaque pathology. *The Journal of clinical investigation* 2007, *117*. 1595-604, DOI: 10.1172/JCI31450.
36. P. Chakrabarty, K. Jansen-West, A. Beccard, C. Ceballos-Diaz, Y. Levites, C. Verbeeck, A. C. Zubair, D. Dickson, T. E. Golde, P. Das, Massive gliosis induced by interleukin-6 suppresses Abeta deposition in vivo: evidence against inflammation as a driving force for amyloid deposition. *FASEB journal : official publication of the Federation of American Societies for Experimental Biology* 2010, *24*. 548-59, DOI: 10.1096/fj.09-141754.
37. (a) J. P. Godbout, R. W. Johnson, Interleukin-6 in the aging brain. *Journal of neuroimmunology* 2004, *147*. 141-4; (b) S. E. Hickman, E. K. Allison, J. El Khoury, Microglial dysfunction and defective beta-amyloid clearance pathways in aging Alzheimer's disease mice. *The Journal of neuroscience : the official journal of the Society for Neuroscience* 2008, *28*. 8354-60, DOI: 10.1523/JNEUROSCI.0616-08.2008.
38. J. Vom Berg, S. Prokop, K. R. Miller, J. Obst, R. E. Kalin, I. Lopategui-Cabezas, A. Wegner, F. Mair, C. G. Schipke, O. Peters, Y. Winter, B. Becher, F. L. Heppner, Inhibition of IL-12/IL-23 signaling reduces Alzheimer's disease-like pathology and cognitive decline. *Nat Med* 2012. DOI: 10.1038/nm.2965.
39. J. M. Craft, D. M. Watterson, E. Hirsch, L. J. Van Eldik, Interleukin 1 receptor antagonist knockout mice show enhanced microglial activation and neuronal damage induced by intracerebroventricular infusion of human beta-amyloid. *Journal of neuroinflammation* 2005, *2*. 15, DOI: 10.1186/1742-2094-2-15.
40. M. Colomiere, A. C. Ward, C. Riley, M. K. Trenerry, D. Cameron-Smith, J. Findlay, L. Ackland, N. Ahmed, Cross talk of signals between EGFR and IL-6R through JAK2/STAT3 mediate epithelial-mesenchymal transition in ovarian carcinomas. *British journal of cancer* 2009, *100*. 134-44, DOI: 10.1038/sj.bjc.6604794.
41. S. L. Montgomery, M. A. Mastrangelo, D. Habib, W. C. Narrow, S. A. Knowlden, T. W. Wright, W. J. Bowers, Ablation of TNF-RI/RII expression in Alzheimer's disease mice leads to an unexpected enhancement of pathology: implications for chronic pan-TNF-alpha suppressive therapeutic strategies in the brain. *The American journal of pathology* 2011, *179*. 2053-70, DOI: 10.1016/j.ajpath.2011.07.001.
42. I. Bulgarelli, L. Tamiazzo, E. Bresciani, D. Rapetti, S. Caporali, D. Lattuada, V. Locatelli, A. Torsello, Desacyl-ghrelin and synthetic GH-secretagogus modulate the production of inflammatory cyotkines in mouse microglia cells stimulated by beta-amyloid fibrils. *Journal of Neuroscience Research* 2009, *87*. 2718-2727, DOI: 19382238.

43. O. Butovsky, A. E. Talpalar, K. Ben-Yaakov, M. Schwartz, Activation of microglia by aggregated beta-amyloid or lipopolysaccharide impairs MHC-II expression and renders them cytotoxic whereas IFN-gamma and IL-4 render them protective. *Molecular and cellular neurosciences* 2005, *29*. 381-93, DOI: 10.1016/j.mcn.2005.03.005.
44. M. Yamamoto, T. Kiyota, M. Horiba, J. L. Buescher, S. M. Walsh, H. E. Gendelman, T. Ikezu, Interferon-gamma and tumor necrosis factor-alpha regulate amyloid-beta plaque deposition and beta-secretase expression in Swedish mutant APP transgenic mice. *The American journal of pathology* 2007, *170*. 680-92, DOI: 10.2353/ajpath.2007.060378.
45. I. R. Turnbull, S. Gilfillan, M. Cella, T. Aoshi, M. Miller, L. Piccio, M. Hernandez, M. Colonna, Cutting edge: TREM-2 attenuates macrophage activation. *Journal of immunology* 2006, *177*. 3520-4.
46. (a) J. N. Ihle, I. M. Kerr, Jaks and Stats in signaling by the cytokine receptor superfamily. *Trends in genetics : TIG* 1995, *11*. 69-74; (b) A. Bernardo, G. Levi, L. Minghetti, Role of the peroxisome proliferator-activated receptor-gamma (PPAR-gamma) and its natural ligand 15-deoxy-Delta12, 14-prostaglandin J2 in the regulation of microglial functions. *The European journal of neuroscience* 2000, *12*. 2215-23.
47. Y. Y. Grinberg, M. E. Dibbern, V. A. Levasseur, R. P. Kraig, Insulin-like growth factor-1 abrogates microglial oxidative stress and TNF-alpha responses to spreading depression. *J Neurochem* 2013, *126*. 662-72, DOI: 10.1111/jnc.12267.
48. A. M. Fernandez, I. Torres-Aleman, The many faces of insulin-like peptide signalling in the brain. *Nature reviews. Neuroscience* 2012, *13*. 225-39, DOI: 10.1038/nrn3209.
49. K. Tahara, H.-D. Kim, J.-J. Jin, J. A. Maxwell, L. Ling, K. Fukuchi, Role of toll-like receptor signalling in A-beta uptake and clearance. *Brain* 2006, *129*. 3006-3019, DOI: 16984903.
50. A. Sierra, A. C. Gottfried-Blackmore, B. S. McEwen, K. Bulloch, Microglia derived from aging mice exhibit an altered inflammatory profile. *Glia* 2007, *55*. 412-24, DOI: 10.1002/glia.20468.
51. J. V. Welser-Alves, R. Milner, Microglia are the major source of TNF-alpha and TGF-beta1 in postnatal glial cultures; regulation by cytokines, lipopolysaccharide, and vitronectin. *Neurochemistry international* 2013, *63*. 47-53, DOI: 10.1016/j.neuint.2013.04.007.
52. J. P. Michaud, M. Halle, A. Lampron, P. Theriault, P. Prefontaine, M. Filali, P. Tribout-Jover, A. M. Lanteigne, R. Jodoin, C. Cluff, V. Brichard, R. Palmantier, A. Pilorget, D. Larocque, S. Rivest, Toll-like receptor 4 stimulation with the detoxified ligand monophosphoryl lipid A improves Alzheimer's disease-related pathology. *Proceedings of the National Academy of Sciences of the United States of America* 2013. DOI: 10.1073/pnas.1215165110.
53. J. Koenigsknecht-Talboo, G. E. Landreth, Microglial phagocytosis induced by fibrillar beta-amyloid and IgGs are differentially regulated by proinflammatory cytokines. *The Journal of neuroscience : the official journal of the Society for Neuroscience* 2005, *25*. 8240-9, DOI: 10.1523/JNEUROSCI.1808-05.2005.
54. F. S. Shie, R. M. Breyer, T. J. Montine, Microglia lacking E Prostanoid Receptor subtype 2 have enhanced Abeta phagocytosis yet lack Abeta-activated neurotoxicity. *The American journal of pathology* 2005, *166*. 1163-72.
55. M. Sastre, I. Dewachter, S. Rossner, N. Bogdanovic, E. Rosen, P. Borghgraef, B. O. Evert, L. Dumitrescu-Ozimek, D. R. Thal, G. Landreth, J. Walter, T. Klockgether, F. van Leuven, M. Heneka, Nonsteroidal anti-inflammatory drugs repress beta-secretase gene promoter activity by the activation of PPARgamma. *Proceedings of the National Academy of Science of the United States of America* 2006, *103*. 443-448, DOI: 16407166.
56. M. T. Heneka, M. Sastre, L. Dumitrescu-Ozimek, A. Hanke, I. Dewachter, C. Kuiperi, K. O'Banion, T. Klockgether, F. Van Leuven, G. E. Landreth, Acute treatment with the PPARgamma agonist pioglitazone and ibuprofen reduces glial inflammation and Abeta1-42 levels in APPV717I transgenic mice. *Brain* 2005, *128*. 1442-53, DOI: 10.1093/brain/awh452.

57. D. J. Loane, B. F. Deighan, R. M. Clarke, R. J. Griffin, A. M. Lynch, M. A. Lynch, Interleukin-4 mediates the neuroprotective effects of rosiglitazone in the aged brain. *Neurobiol Aging* 2009, *30*. 920-31, DOI: 10.1016/j.neurobiolaging.2007.09.001.
58. M. Yamanaka, T. Ishikawa, A. Griep, D. Axt, M. P. Kummer, M. T. Heneka, PPARgamma/RXRalpha-induced and CD36-mediated microglial amyloid-beta phagocytosis results in cognitive improvement in amyloid precursor protein/presenilin 1 mice. *The Journal of neuroscience : the official journal of the Society for Neuroscience* 2012, *32*. 17321-31, DOI: 10.1523/JNEUROSCI.1569-12.2012.
59. N. Zelcer, N. Khanlou, R. Clare, Q. Jiang, E. G. Reed-Geaghan, G. E. Landreth, H. V. Vinters, P. Tontonoz, Attenuation of neuroinflammation and Alzheimer's disease pathology by liver x receptors. *Proceedings of the National Academy of Sciences of the United States of America* 2007, *104*. 10601-6, DOI: 10.1073/pnas.0701096104.
60. H. Fan, Y. Guo, X. Liang, Y. Yuan, X. Qi, M. Wang, J. Ma, H. Zhou, Hydrogen sulfide protects against amyloid beta-peptide induced neuronal injury via attenuating inflammatory responses in a rat model. *Journal of biomedical research* 2013, *27*. 296-304, DOI: 10.7555/JBR.27.20120100.
61. B. M. Necela, W. Su, E. A. Thompson, Toll-like receptor 4 mediates cross-talk between peroxisome proliferator-activated receptor gamma and nuclear factor-kappaB in macrophages. *Immunology* 2008, *125*. 344-58, DOI: 10.1111/j.1365-2567.2008.02849.x.
62. (a) J. Tan, T. Town, D. Paris, T. Mori, Z. Suo, F. Crawford, M. P. Mattson, R. A. Flavell, M. Mullan, Microglial activation resulting from CD40-CD40L interaction after beta-amyloid stimulation. *Science* 1999, *286*. 2352-5; (b) J. Tan, T. Town, F. Crawford, T. Mori, A. DelleDonne, R. Crescentini, D. Obregon, R. A. Flavell, M. J. Mullan, Role of CD40 ligand in amyloidosis in transgenic Alzheimer's mice. *Nature neuroscience* 2002, *5*. 1288-93, DOI: 10.1038/nn968.
63. E. Shimizu, K. Kawahara, M. Kajizono, M. Sawada, H. Nakayama, IL-4-induced selective clearance of oligomeric beta-amyloid peptide(1-42) by rat primary type 2 microglia. *Journal of immunology* 2008, *181*. 6503-13.
64. (a) R. Guerreiro, A. Wojtas, J. Bras, M. Carrasquillo, E. Rogaeva, E. Majounie, C. Cruchaga, C. Sassi, J. S. Kauwe, S. Younkin, L. Hazrati, J. Collinge, J. Pocock, T. Lashley, J. Williams, J. C. Lambert, P. Amouyel, A. Goate, R. Rademakers, K. Morgan, J. Powell, P. St George-Hyslop, A. Singleton, J. Hardy, G. the Alzheimer Genetic Analysis, TREM2 Variants in Alzheimer's Disease. *The New England journal of medicine* 2012. DOI: 10.1056/NEJMoa1211851; (b) T. Jonsson, H. Stefansson, D. S. Ph, I. Jonsdottir, P. V. Jonsson, J. Snaedal, S. Bjornsson, J. Huttenlocher, A. I. Levey, J. J. Lah, D. Rujescu, H. Hampel, I. Giegling, O. A. Andreassen, K. Engedal, I. Ulstein, S. Djurovic, C. Ibrahim-Verbaas, A. Hofman, M. A. Ikram, C. M. van Duijn, U. Thorsteinsdottir, A. Kong, K. Stefansson, Variant of TREM2 Associated with the Risk of Alzheimer's Disease. *The New England journal of medicine* 2012. DOI: 10.1056/NEJMoa1211103.
65. (a) K. Takahashi, C. D. Rochford, H. Neumann, Clearance of apoptotic neurons without inflammation by microglial triggering receptor expressed on myeloid cells-2. *The Journal of experimental medicine* 2005, *201*. 647-57, DOI: 10.1084/jem.20041611; (b) H. Neumann, K. Takahashi, Essential role of the microglial triggering receptor expressed on myeloid cells-2 (TREM2) for central nervous tissue immune homeostasis. *Journal of neuroimmunology* 2007, *184*. 92-9, DOI: 10.1016/j.jneuroim.2006.11.032.
66. M. Colonna, TREMs in the immune system and beyond. *Nature reviews. Immunology* 2003, *3*. 445-53, DOI: 10.1038/nri1106.

67. (a) C. L. Hsieh, M. Koike, S. C. Spusta, E. C. Niemi, M. Yenari, M. C. Nakamura, W. E. Seaman, A role for TREM2 ligands in the phagocytosis of apoptotic neuronal cells by microglia. *J Neurochem* 2009, *109*. 1144-56, DOI: 10.1111/j.1471-4159.2009.06042.x; (b) B. Melchior, A. E. Garcia, B. K. Hsiung, K. M. Lo, J. M. Doose, J. C. Thrash, A. K. Stalder, M. Staufenbiel, H. Neumann, M. J. Carson, Dual induction of TREM2 and tolerance-related transcript, Tmem176b, in amyloid transgenic mice: implications for vaccine-based therapies for Alzheimer's disease. *ASN neuro* 2010, *2*. e00037, DOI: 10.1042/AN20100010.

68. K. Takahashi, M. Prinz, M. Stagi, O. Chechneva, H. Neumann, TREM2-transduced myeloid precursors mediate nervous tissue debris clearance and facilitate recovery in an animal model of multiple sclerosis. *PLoS medicine* 2007, *4*. e124, DOI: 10.1371/journal.pmed.0040124.

69. J. A. Hamerman, J. R. Jarjoura, M. B. Humphrey, M. C. Nakamura, W. E. Seaman, L. L. Lanier, Cutting edge: inhibition of TLR and FcR responses in macrophages by triggering receptor expressed on myeloid cells (TREM)-2 and DAP12. *Journal of immunology* 2006, *177*. 2051-5.

70. R. T. Mott, G. Ait-Ghezala, T. Town, T. Mori, M. Vendrame, J. Zeng, J. Ehrhart, M. Mullan, J. Tan, Neuronal expression of CD22: novel mechanism for inhibiting microglial proinflammatory cytokine production. *Glia* 2004, *46*. 369-79, DOI: 10.1002/glia.20009.

71. A. Lyons, E. J. Downer, S. Crotty, Y. M. Nolan, K. H. Mills, M. A. Lynch, CD200 ligand receptor interaction modulates microglial activation in vivo and in vitro: a role for IL-4. *The Journal of neuroscience : the official journal of the Society for Neuroscience* 2007, *27*. 8309-13, DOI: 10.1523/JNEUROSCI.1781-07.2007.

72. S. Zhang, H. Cherwinski, J. D. Sedgwick, J. H. Phillips, Molecular mechanisms of CD200 inhibition of mast cell activation. *Journal of immunology* 2004, *173*. 6786-93.

73. D. G. Walker, J. E. Dalsing-Hernandez, N. A. Campbell, L. F. Lue, Decreased expression of CD200 and CD200 receptor in Alzheimer's disease: a potential mechanism leading to chronic inflammation. *Experimental neurology* 2009, *215*. 5-19, DOI: 10.1016/j.expneurol.2008.09.003.

74. (a) J. F. Bazan, K. B. Bacon, G. Hardiman, W. Wang, K. Soo, D. Rossi, D. R. Greaves, A. Zlotnik, T. J. Schall, A new class of membrane-bound chemokine with a CX3C motif. *Nature* 1997, *385*. 640-4, DOI: 10.1038/385640a0; (b) J. K. Harrison, Y. Jiang, S. Chen, Y. Xia, D. Maciejewski, R. K. McNamara, W. J. Streit, M. N. Salafranca, S. Adhikari, D. A. Thompson, P. Botti, K. B. Bacon, L. Feng, Role for neuronally derived fractalkine in mediating interactions between neurons and CX3CR1-expressing microglia. *Proceedings of the National Academy of Sciences of the United States of America* 1998, *95*. 10896-901.

75. A. E. Cardona, E. P. Pioro, M. E. Sasse, V. Kostenko, S. M. Cardona, I. M. Dijkstra, D. Huang, G. Kidd, S. Dombrowski, R. Dutta, J. C. Lee, D. N. Cook, S. Jung, S. A. Lira, D. R. Littman, R. M. Ransohoff, Control of microglial neurotoxicity by the fractalkine receptor. *Nature neuroscience* 2006, *9*. 917-24, DOI: 10.1038/nn1715.

76. S. Lee, N. H. Varvel, M. E. Konerth, G. Xu, A. E. Cardona, R. M. Ransohoff, B. T. Lamb, CX3CR1 deficiency alters microglial activation and reduces beta-amyloid deposition in two Alzheimer's disease mouse models. *The American journal of pathology* 2010, *177*. 2549-62, DOI: 10.2353/ajpath.2010.100265.

77. R. S. Duan, X. Yang, Z. G. Chen, M. O. Lu, C. Morris, B. Winblad, J. Zhu, Decreased fractalkine and increased IP-10 expression in aged brain of APP(swe) transgenic mice. *Neurochemical research* 2008, *33*. 1085-9, DOI: 10.1007/s11064-007-9554-z.

78. T. F. Pais, C. Figueiredo, R. Peixoto, M. H. Braz, S. Chatterjee, Necrotic neurons enhance microglial neurotoxicity through induction of glutaminase by a MyD88-dependent pathway. *Journal of neuroinflammation* 2008, *5*. 43, DOI: 10.1186/1742-2094-5-43.

79. P. Davies, A. J. Maloney, Selective loss of central cholinergic neurons in Alzheimer's disease. *Lancet* 1976, *2*. 1403.

80. (a) R. D. Shytle, T. Mori, K. Townsend, M. Vendrame, N. Sun, J. Zeng, J. Ehrhart, A. A. Silver, P. R. Sanberg, J. Tan, Cholinergic modulation of microglial activation by alpha 7 nicotinic receptors. *J Neurochem* 2004, *89*. 337-43, DOI: 10.1046/j.1471-4159.2004.02347.x; (b) R. De Simone, M. A. Ajmone-Cat, D. Carnevale, L. Minghetti, Activation of alpha7 nicotinic acetylcholine receptor by nicotine selectively up-regulates cyclooxygenase-2 and prostaglandin E2 in rat microglial cultures. *Journal of neuroinflammation* 2005, *2*. 4, DOI: 10.1186/1742-2094-2-4.

81. T. Suzuki, I. Hide, A. Matsubara, C. Hama, K. Harada, K. Miyano, M. Andra, H. Matsubayashi, N. Sakai, S. Kohsaka, K. Inoue, Y. Nakata, Microglial alpha7 nicotinic acetylcholine receptors drive a phospholipase C/IP3 pathway and modulate the cell activation toward a neuroprotective role. *J Neurosci Res* 2006, *83*. 1461-70, DOI: 10.1002/jnr.20850.

82. W. J. de Jonge, L. Ulloa, The alpha7 nicotinic acetylcholine receptor as a pharmacological target for inflammation. *British journal of pharmacology* 2007, *151*. 915-29, DOI: 10.1038/sj.bjp.0707264.

83. J. H. Moon, S. Y. Kim, H. G. Lee, S. U. Kim, Y. B. Lee, Activation of nicotinic acetylcholine receptor prevents the production of reactive oxygen species in fibrillar beta amyloid peptide (1-42)-stimulated microglia. *Experimental & molecular medicine* 2008, *40*. 11-8, DOI: 10.3858/emm.2008.40.1.11.

84. H. G. Kim, M. Moon, J. G. Choi, G. Park, A. J. Kim, J. Hur, K. T. Lee, M. S. Oh, Donepezil inhibits the amyloid-beta oligomer-induced microglial activation in vitro and in vivo. *Neurotoxicology* 2013. DOI: 10.1016/j.neuro.2013.10.004.

85. H. J. Kim, M. H. Lee, H. S. Park, M. H. Park, S. W. Lee, S. Y. Kim, J. Y. Choi, H. I. Shin, H. J. Kim, H. M. Ryoo, Erk pathway and activator protein 1 play crucial roles in FGF2-stimulated premature cranial suture closure. *Developmental dynamics : an official publication of the American Association of Anatomists* 2003, *227*. 335-46, DOI: 10.1002/dvdy.10319.

86. I. K. Puri, L. Li, Mathematical modeling for the pathogenesis of Alzheimer's disease. *PloS one* 2010, *5*. e15176, DOI: 10.1371/journal.pone.0015176.

87. J. T. Rogers, L. M. Leiter, J. McPhee, C. M. Cahill, S. S. Zhan, H. Potter, L. N. Nilsson, Translation of the alzheimer amyloid precursor protein mRNA is up-regulated by interleukin-1 through 5'-untranslated region sequences. *J Biol Chem* 1999, *274*. 6421-31.

# Figure

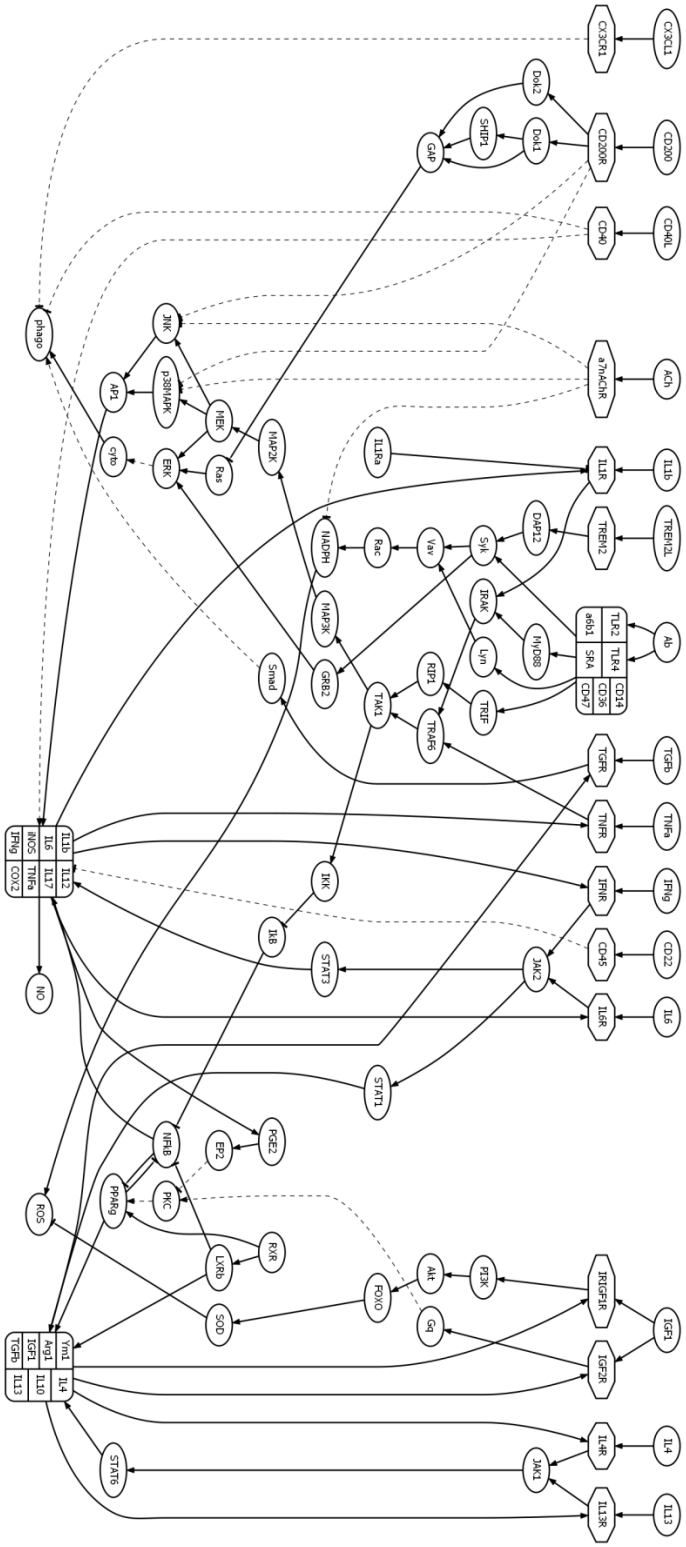


Figure 1. Model diagram. Dashed lines connote indirect connections. Arrows and tees connote positive and negative connections, respectively. For abbreviations see Table S1.

**Tables**

Table 1. Truth table. The input elements in the truth table are the inflammatory stimuli Ab and LPS, the compounds rosi and retino, and the initial levels of key cytokines: IFNgini, IL4ini, and IGF1ini. The output elements are those for which consistent experimental results have been reported. The young and old cases are distinguished, respectively, by the presence or absence of the neuronal factors ACh, CD22, CD200, CX3CL1, and TREM2L. All element levels are nonzero integers representing relative activities. Numerals in bold reflect changes in activity levels that have been observed experimentally and that must be matched by the outputs of both the Maude and MATLAB versions of the microglia signaling model. Numerals in plain font are those for which no matching experimental data yet exist. Italic numerals represent the output levels of two stable states reached by the Maude version that match neither observation nor MATLAB output (see Results).

| | **inputs** | | | | | | | | **outputs** | | | | | | | | | |
|---|---|---|---|---|---|---|---|---|---|---|---|---|---|---|---|---|---|---|
| **row** | Ab | LPS | IFNgini | IL4ini | IGF1ini | rosi | retino | **age** | IL1b | TNFa | ROS | phago | Ym1 | Arg1 | IL4 | IL10 | TGFb | IGF1 |
| **1** | 0 | 0 | 5 | 5 | 5 | 0 | 0 | | **5** | **5** | **5** | **5** | **5** | **5** | **5** | **5** | **5** | **5** |
| **2** | 1 | 0 | 5 | 5 | 5 | 0 | 0 | | **7** | **7** | **7** | **7** | **7** | **5** | 7 | **7** | **7** | **3** |
| **3** | 0 | 1 | 5 | 5 | 5 | 0 | 0 | **young** | **7** | **7** | 7 | 7 | 7 | 5 | 7 | **7** | **7** | **3** |
| **4** | 0 | 0 | 8 | 5 | 5 | 0 | 0 | | 7 | **7** | 5 | 7 | 7 | 5 | 7 | 7 | 7 | **3** |
| **5a** | 0 | 0 | 5 | 8 | 5 | 0 | 0 | | *5* | *5* | *5* | *7* | *7* | *5* | *7* | *7* | *7* | *5* |
| **5b** | " | " | " | " | " | " | " | | 3 | **3** | 3 | 7 | 7 | 5 | 7 | 7 | 7 | **7** |
| **6** | 0 | 0 | 5 | 5 | 5 | 0 | 0 | | **7** | **7** | 5 | **3** | 7 | 5 | 7 | 7 | 7 | 3 |
| **7** | 1 | 0 | 5 | 5 | 5 | 0 | 0 | | **7** | **7** | 7 | **3** | 7 | **5** | **7** | **7** | **7** | 3 |
| **8** | 0 | 1 | 5 | 5 | 5 | 0 | 0 | | **7** | **7** | 7 | 3 | 7 | 5 | 7 | **7** | **7** | 3 |
| **9** | 1 | 1 | 5 | 5 | 5 | 0 | 0 | | **7** | 7 | 7 | **3** | 3 | **3** | **3** | 3 | 3 | 3 |
| **10a** | 1 | 1 | 5 | 8 | 5 | 0 | 0 | **old** | *7* | *7* | *7* | *3* | *3* | *3* | *3* | *3* | *3* | *3* |
| **10b** | " | " | " | " | " | " | " | | 3 | 3 | 5 | **7** | 7 | 5 | 7 | 7 | 7 | **7** |
| **11** | 0 | 0 | 5 | 5 | 8 | 0 | 0 | | 3 | **3** | **3** | 7 | 7 | 5 | 7 | 7 | 7 | 7 |
| **12** | 1 | 0 | 5 | 5 | 5 | 1 | 0 | | **3** | **3** | 5 | **7** | 7 | 5 | **7** | 7 | 7 | 7 |
| **13** | 1 | 0 | 5 | 5 | 5 | 0 | 1 | | 3 | 3 | 5 | **7** | 7 | 5 | 7 | 7 | 7 | 7 |

Table 2. Temporal-logic model-checking in the young case with Ab present.

| row | proposition | value |
|---|---|---|
| **1** | IL1b is always high and IFNg is always high | true |
| **2** | NFkB is always high | true |
| **3** | IL4 is always high or IGF1 is always low | false |
| **4** | IL4 is eventually high and IGF1 is eventually low | true |
| **5** | PPARg is never greater than base | true |
| **6** | STAT1 is always high or STAT6 is always high | false |
| **7** | STAT1 is eventually high and STAT6 is eventually high | true |
| **8** | IL4 is not high or IGF1 is not low until STAT6 is high | false |
| **9** | IL4 is not high and IGF1 is not low until STAT1 is high | true |
| **10** | STAT1 being high implies that IL4 is high and IGF1 is low | true |
| **11** | ROS is always high | true |
| **12** | phago is always high | false |
| **13** | phago is eventually high | true |
| **14** | Smad is always high | false |
| **15** | Smad is eventually high | true |
| **16** | Smad is not high until STAT1 is high | true |
| **17** | STAT1 being high implies phago is high | false |
| **18** | STAT1 being high leads to phago being high | true |
| **19** | Smad being high implies that phago is high | true |

Table 3. Temporal-logic model-checking in the young case with augmented initial IL4.

| row | proposition | value |
|---|---|---|
| **1** | IL1b is always low and IGF1 is always high | false |
| **2** | IL1b is always low | false |
| **3** | IL1b is eventually low | false |
| **4** | IGF1 is always high | false |
| **5** | IGF1 is eventually high | true |
| **6** | STAT6 above high implies that IGF1 is high | true |
| **7** | IGF1 being high implies that IGF1 remains high | false |
| **8** | IL1b is not low until IGF1 is high | true |
| **9** | IGF1 being high leads to IL1b being low | false |
| **10** | AP1 being low implies that AP1 remains low | true |
| **11** | STAT3 being low implies that STAT3 remains low | true |
| **12** | NFkB being low implies that NFkB remains low | true |
| **13** | IL1b being low implies that AP1 is low | false |
| **14** | IL1b being low implies that STAT3 is low | false |
| **15** | IL1b being low implies that NFkB is low | true |
| **16** | NFkB is not low until IGF1 is high | true |
| **17** | PPARg is not above high until IGF1 is high | true |
| **18** | PKC is not above high until IGF1 is high | true |
| **19** | Gq is not high until IGF1 is high | true |
| **20** | Gq being high implies that IL1b is low | true |
| **21** | IGF1 being high leads to Gq being high | false |
| **22** | Gq being high implies that IGF1 is high | true |
| **23** | Gq being high implies that Gq remains high | true |

Table 4. Temporal-logic model-checking in the old case without Ab or LPS.

| row | proposition | value |
|---|---|---|
| **1** | NFkB is always high | false |
| **2** | NFkB is eventually high | true |
| **3** | STAT3 is always high | false |
| **4** | STAT3 is eventually high | true |
| **5** | AP1 is always above base | true |
| **6** | p38MAPK is always above base | true |
| **7** | JNK is always above base | true |
| **8** | IL1b is always high | true |
| **9** | IFNg is always high | true |

Table 5. Temporal-logic model-checking in the old case with Ab and LPS.

| row | proposition | value |
|---|---|---|
| **1** | IL1b is always high and IFNg is always high | true |
| **2** | IL4 is always low and IGF1 is always low | false |
| **3** | IL4 is always low | true |
| **4** | IGF1 is eventually low | true |
| **5** | NFkB is always above high | true |
| **6** | NFkB above high implies IL1b is high and IFNg is high | true |
| **7** | PPARg is always low | true |
| **8** | NFkB above high implies PPARg is low | true |
| **9** | PPARg being low implies that IL4 is low | true |
| **10** | PPARg being low implies that IGF1 is low | false |
| **11** | STAT1 is always high | false |
| **12** | STAT1 is eventually high | true |
| **13** | STAT6 is always low | false |
| **14** | STAT6 is eventually low | true |
| **15** | IGF1 is not low until STAT6 is low | false |
| **16** | IGF1 is not low until STAT1 is high | true |
| **17** | STAT1 is not high until IFNg is high or IL6 is high | true |
| **18** | IGF1 is not low until IFNg is high or IL6 is high | true |

Table 6. Model-checking in the old case with Ab, LPS, and augmented initial IL4.

| row | proposition | value |
|---|---|---|
| **1** | STAT6 above high implies that IGF1 is high | true |
| **2** | Gq being high implies that IGF1 is high | true |
| **3** | Gq being high implies that Gq remains high | true |
| **4** | PKC is not above high until IGF1 is high | true |
| **5** | PPARg is not above high until IGF1 is high | true |
| **6** | NFkB is not low until IGF1 is high | true |
| **7** | IL1b being low implies that NFkB is low | true |
| **8** | IL10 being high implies that PPARg is above high | true |
| **9** | ROS is high and not at base until IGF1 is high | true |
| **10** | TGFb being high implies that PPARg is above high | true |
| **11** | Smad being high implies that TGFb is high | true |
| **12** | Smad being high implies that phago is high | true |